SECURITY CLASSIFICATION OF THIS PAGE (When Data Entered)

REPORT DOCUMENTATION PAGE

READ INSTRUCTIONS

ADA005399

1. REPORT NUMBER
AFAPL-TR-74 -90

2. GOVT ACCESSION NO

4. TITLE (and Subtitle)
Dump Combustor Parametric Investigation

5. TYPE OF REPORT & PERIOD COVERED
Final

6. PERFORMING ORG. REPORT NUMBER

7. AUTHOR(s)
F.D. Stull, R.R. Craig, J.T. Hojnacki

8. CONTRACT OR GRANT NUMBER(s)

9. PERFORMING ORGANIZATION NAME AND ADDRESS
AF Aero Propulsion Laboratory (RJT)
Wright-Patterson AFB, Ohio

10. PROGRAM ELEMENT, PROJECT, TASK AREA & WORK UNIT NUMBERS
3012-12-08

11. CONTROLLING OFFICE NAME AND ADDRESS
Air Force Aero Propulsion Laboratory (RJT)
Wright-Patterson AFB, Ohio

12. REPORT DATE
November 1974

13. NUMBER OF PAGES
63

14. MONITORING AGENCY NAME & ADDRESS(if different from Controlling Office)

15. SECURITY CLASS. (of this report)
Unclassified

15a. DECLASSIFICATION/DOWNGRADING SCHEDULE

16. DISTRIBUTION STATEMENT (of this Report)
Approved for Public Release, Distribution Unlimited.

17. DISTRIBUTION STATEMENT (of the abstract entered in Block 20, if different from Report)

18. SUPPLEMENTARY NOTES
Report is an expansion of a paper presented at the ASME Joint Fluids Engineering and CSME Conference, Montreal, Quebec, May 13-15, 1974.

19. KEY WORDS (Continue on reverse side if necessary and identify by block number)
Combustors, Ramjet Combustion, Dump Combustors, Pressure Scaling, Combustion Instability, Shelldyne-H Fuel.

20. ABSTRACT (Continue on reverse side if necessary and identify by block number)
A series of scale model coaxial dump combustors from 2" to 5" D were tested on a thrust stand with JP-4 fuel over a wide range of ramjet test conditions. Baseline conditions were selected to approximate "pressure scaling criteria" in which chamber pressure times combustor diameter remains constant. JP-4 fuel was injected perpendicular to the airstream from eight plane tube injectors. Fuel/air ratio, chamber pressure and nozzle throat diameter were varied for each size chamber. Lean blow-out limit, combustion efficiency, combustor pressure drop, and combustion instability characteristics were obtained for each test point.

DD FORM 1 JAN 73 1473 EDITION OF 1 NOV 65 IS OBSOLETE

PRICES SUBJECT TO CHANGE

SECURITY CLASSIFICATION OF THIS PAGE (When Data Entered)

REPRODUCED BY: NTIS
U.S. Department of Commerce
National Technical Information Service
Springfield, Virginia 22161

Combustion instability was encountered in all tests when the ratio of the exit throat area to combustor area was less than 0.2. Under these conditions, the frequency and amplitude of the pressure oscillation was also recorded.

A parametric study was then conducted around the 5" D baseline configuration in which combustor length-to-diameter ratio (L/D), characteristic length (L*), inlet temperature, and number of fuel injectors were varied. A strong effect on combustion efficiency was noted for L/D's less than 4.5. Combustion efficiency and combustor pressure losses were determined from each of these runs and compared to several existing correlations.

Additional tests were then conducted using Shelldyne-H fuel. Little difference was noted in combustion efficiency between Shelldyne and JP-4 when tested under baseline conditions. However, at low inlet temperatures of around 750°R, combustion efficiency decreased rapidly for Shelldyne as fuel/air ratio was increased. Several additives that had shown promise from shock tube studies were used with Shelldyne in an attempt to increase combustion efficiency.

GENERAL DISCLAIMER

This document may be affected by one or more of the following statements

- This document has been reproduced from the best copy furnished by the sponsoring agency. It is being released in the interest of making available as much information as possible.
- This document may contain data which exceeds the sheet parameters. It was furnished in this condition by the sponsoring agency and is the best copy available.
- This document may contain tone-on-tone or color graphs, charts and/or pictures which have been reproduced in black and white.
- This document is paginated as submitted by the original source.
- Portions of this document are not fully legible due to the historical nature of some of the material. However, it is the best reproduction available from the original submission.

FOREWORD

This report was prepared by the Ramjet Technology Branch, Ramjet Engine Division, Air Force Aero Propulsion Laboratory, Wright-Patterson Air Force Base, Ohio 45433. The work was accomplished under Project 3012, "Ramjet Technology," and Task 301212, "In-House Ramjet Technology."

The report covers work performed during the time period of March 1973 through January 1974.

This report was submitted for publication by the authors 28 June 1974.

TABLE OF CONTENTS

SECTION		PAGE
I	INTRODUCTION	1
II	EXPERIMENTAL PROCEDURE	2
	1. Test Hardware	2
	2. Test Rig	3
	3. Combustion Efficiency Calculation	3
III	DISCUSSION AND RESULTS	7
	1. Combustor Scaling	7
	2. Combustor L/D	9
	3. Combustor L*	10
	4. Combustor Dump Area	10
	5. Inlet Temperature	10
	6. Number of Fuel Injectors	11
	7. Type of Fuel	11
	8. Fuel Additives	12
	9. Flame Stabilization	12
	10. Generalized Performance	13
	11. Combustor Pressure Losses	14
IV	CONCLUSIONS	16
V	REFERENCES	17
VI	APPENDIX A	19
VII	APPENDIX B	23

Preceding page blank

LIST OF FIGURES

FIGURE		PAGE
1.	Combustor Scaling Relationships	31
2.	Sketch of Test Hardware	32
3.	Scale Model Combustors	33
4.	Ideal Temperature Rise	34
5.	Air Specific Stream Thrust	35
6.	Air Specific Stream Thrust for Combustion Gases	36
7.	Pressure Scaling Tests	37
8.	Scale Model Test f/a = .025	38
9.	Scale Model Test f/a = .040	39
10.	Scale Model Test f/a = .055	40
11.	Effects of Combustor L/D	41
12.	Constant Combustor L* Tests	42
13.	Effects of Dump Area Ratio	43
14.	Effects of Inlet Air Temperature	44
15.	Effects of Injector Number	45
16.	Effects of Fuel Type	46
17.	Effects of Fuel Additives to Shelldyne	47
18.	Stability Data Correlation	48
19.	Attempted Performance Correlations	49
20.	Burner Severity Parameter	50
21.	Characteristic Length Correlation	51
22.	Stability Correlation	52
23.	Modified Longwell Parameter	53

LIST OF FIGURES (cont'd)

FIGURE		PAGE
24.	Pressure Loss Correlation Parameter	54
25.	Comparison of Several Pressure Loss Parameters	55
26.	Mass Flow Parameter for Combustion Gases	56

SYMBOLS

A	Area - in^2
C_{D_B}	Burner Drag Coefficient
D	Diameter - in
de	Equivalent Dimension
F	Stream Thrust - lb
f	Frequency - cycles/sec
f/a	Fuel-to-Air Ratio
g	Gravitational Constant - 32.174 ft/sec^2
L	Length of Combustor - in
L^*	Combustor Characteristic Length
M	Mach Number
$\mathbf{M}$	Molecular Weight
N_D	Dump Pressure Loss Parameter
P	Pressure - lb/in^2
$\mathcal{R}$	Universal Gas Constant - 1545 ft-lb/lb mole-R°
Sa	Air Specific Stream Thrust
T	Temperature - °R
V	Velocity - ft/sec
$\dot{W}$	Weight flow - lb/sec
γ	Ratio of Specific Heats
η_c	Combustion Efficiency
ϕ	Equivalence Ratio

SUBSCRIPTS

2	Inlet to Combustor
3	Beginning of Combustor
4	End of Combustor
*	Sonic Point
c	Combustion Chamber
e	Nozzle Exit
T	Stagnation Conditions

SECTION I

INTRODUCTION

Current volume limited ramjet designs employ dump combustors. In this engine system the booster rocket is integrated into the ramjet combustor to conserve missile volume. Such combustors do not contain combustor liners or conventional flameholders within the combustion region and must depend to a large extent upon recirculation zones formed by the sudden enlargement area between the inlet duct and the combustor chamber.

Many combustors have been successfully developed over the years which have demonstrated adequate performance for limited operating conditions. Because of the specific nature of these prior designs, no real data base exists on the scaling of dump combustors or on systematically varying key combustor geometries and test conditions. This report covers in-house combustion efforts conducted at the Air Force Aero Propulsion Laboratory, in an attempt to establish some of the design data base needed to support future ramjet developments. The results are applicable to coaxial dump combustors without flameholders and includes both JP-4 and Shelldyne data. A similar program involving the use of flameholders in the inlet duct is being conducted and will be reported in a future report.

SECTION II

EXPERIMENTAL PROCEDURE

Test Hardware

The scale model test hardware was essentially designed according to "pressure scaling" relationships [1, 2], in which overall geometric similarity was maintained, see Fig. 1. The fuel injectors consisted of 8 equally spaced, fixed orifice, wall injectors located 2.5 inches upstream of the dump section. This distance was determined from previous fuel injection studies [3] and was held constant. The orifice diameter was scaled so that, at a fuel/air ratio of .055, the ratio of penetration distance to inlet diameter was a constant value of .16. Cross-stream injection was used throughout the test program.

Combustors with diameters of 2", 3", 4", and 5" were fabricated from Schedule 40 (1/4" wall) stainless steel pipe flanged at both ends. The coaxial inlet duct was fabricated from similar stainless steel pipe with a diameter equal to 1/2 that of the combustor, see Fig. 2. An assortment of convergent exit nozzles varying from 3/4" to 4 1/4" allowed the scale models to be tested at essentially constant combustor velocity conditions for the pressure scaling tests. Fig. 3 is a photograph of the four scaled combustors with one set of exit nozzles. Combustor L/D's for each of these baseline models is 3. In addition, other length combustors were available with the 5" D hardware so that combustor L/D could be varied from 1.5 to 6. By combining the various exit nozzle sizes with the different length combustors, conditions of essentially constant L* but varying L/D's could be achieved.

Likewise by interchanging the various inlet ducts with a given combustor diameter, the effects of varying sudden dump expansion ratio could be observed.

Test Rig

The combustor hardware consisting of the inlet duct and combustor chamber were mounted directly on a thrust stand from which combustion efficiency was obtained. Heated air was supplied from the 300 psi Laboratory air supply system through an indirect fired gas furnace and was controlled by a 3" high temperature air valve. The inlet air temperature, measured with chromel-alumel thermocouples, was varied from 750°R to 1250°R during these tests. An orifice plate metered the air flow rate which was varied from about .5 lb/sec to over 6 lb/sec. Fuel flow to the fuel injectors was measured by a turbine type flow meter. Unbonded strain gage pressure transducers were used for monitoring the inlet duct and combustor chamber static pressures as well as detecting pressure fluctuations. A Baldwin Lima Hamilton load cell type U3XX was mounted to the thrust stand.

Data from all of the instrumentation was recorded on magnetic tape for computer processing. A Hewlett-Packard 2012B digital data acquisition system acquired the data at a rate of 15 channels per second. For all tests, data was recorded for the cold flow just prior to igniting the fuel/air mixture and continued until the combustor chamber glowed red and the fuel flow terminated.

Combustion Efficiency Calculation

There are many definitions used in the propulsion industry for combustion efficiency. The definition of combustion efficiency, η_c, used in this report is

$$\eta_c = \Delta T_t / \Delta T_{t_i}$$

where ΔT_t is the stagnation temperature rise computed from engine thrust measurements and ΔT_{t_i} is the ideal total temperature rise computed from equilibrium chemistry calculations for the measured fuel-to-air ratio, f/a.

The ideal temperature rise for several hydrocarbon fuels and additives is shown in Fig. 4. Here the abscissas variable is equivalence ratio, ϕ, defined as

$$\phi = \frac{f/a}{(f/a)_{stoichiometric}}$$

Data for only one initial temperature, T_{T2}, and one chamber pressure, P_{T4}, are shown. The temperature rise curve does vary with T_{T2} but varies only weakly with pressure. These data are stored in a data reduction program as a two dimensional array with ϕ and T_{T2} as the independent variables.

The thrust stand used in this test program was designed so that all of the inlet air momentum is removed from the incoming air before it reaches the thrust stand. The measured thrust is then only a function of the flow momentum leaving the nozzle of the combustion chamber. Thus

$$Fe = \frac{We}{g} Ve + PeAe$$

where $\dot{W}e$ is the total weight flow through the engine, Ve is the nozzle exit velocity, Pe is the nozzle exit pressure and Ae the nozzle exit area.

If an air specific stream thrust, Sa_e is defined as

$$Sa_e = F_e/\dot{W}_2$$

where $\dot{W}_2$ is the air flow entering the combustor, one obtains

$$Sa_e = (1+f/a)\sqrt{\frac{\mathcal{R}}{Meg} T_{t_e}} \frac{(1+\gamma Me^2)}{M_e \sqrt{\gamma} (1+\frac{\gamma-1}{2} M_e^2)^{1/2}} \qquad (1)$$

where $\mathcal{R}$ is the universal gas constant, γ is the ratio of specific heats, M_e the molecular weight and M_e the Mach number of the flow at the nozzle exit. Since only the difference in the thrust of tne flow with the fuel on and the fuel off

is measured, this can be related to Sa_e as follows:

$$\Delta F = \dot{W}_2 \, (Sa_e - Sa_{air})$$

then

$$Sa_e = \frac{\Delta F}{\dot{W}_2} + Sa_{air} \qquad (2)$$

Sa_{air} is easily obtained from equation (1) since one knows T_{T_e} and M_e when no combustion is occurring. The Mach number effect in equation (1) is eliminated by using a sonic orifice for the nozzle and Sa_{air} can be computed very accurately from

$$Sa_{air} = 2.39 \sqrt{T_{T_2}}$$

Under certain operating conditions, since the flow is exhausted to the atmosphere, the nozzle will be choked when combustion is occurring but becomes unchoked when the fuel is turned off. Thus Sa_{air} will increase as the flow becomes more subsonic, as shown in Fig. 5. However, this increase is not a strong function of Mach number near sonic conditions, increasing only 2% when the Mach number drops to 0.8. This effect is not included in the calculations and under these conditions the computed combustion efficiencies will be slightly pessimistic.

With the value of air specific stream thrust obtained from equation 2, one must now determine a value for T_{T_e}. From equation (1) one observes that if the ratio $Sa_e/(1+f/a) \sqrt{T_{T_e}}$ is formed, the result would only be a weakly varying function of γ and M_e for a sonic nozzle. Using the NASA thermochemical program, [4], the ratio is computed and plotted versus T_{T_e}. The results are shown in Fig. 6 for Shelldyne-H fuel, more commonly designated as RJ-5. Also shown is a curve

for JP-4 at 5 atmospheres. It is interesting to note that if the RJ-5 curves are used to reduce data for JP-4 a maximum error of 2% in combustion efficiency would be incurred and demonstrates the relative insensitivity of this parameter to temperature and fuel type.

These data are input as a two-dimensional table into a data reduction program with pressure and total temperature, T_{T_e}, as the independent variables. A first guess of 2.43 is used for this ratio and with the measured values of f/a and Sa_e, a total temperature is computed. This temperature is then used to obtain a better value for the ratio $Sa_e/(1+f/a)\sqrt{T_{T_e}}$ from the table and the final temperature computed.

The temperature computed in this manner is not only a measure of chemical efficiency of the combustor but it is also a measure of how well the flow is mixed before it exits the nozzle. For example, if one locally burned all of the fuel stoichiometrically at 100% efficiency when the overall fuel-air ratio was 40% of stoichiometric and failed to mix these products with the colder stream, the combustion efficiency deduced from the thrust measurement would only be 66%.

SECTION III

DISCUSSION & RESULTS

Combustor Scaling

All of the scale combustor models were tested at baseline conditions which approximated the "pressure scaling" criteria. To accomplish this, the air flow was adjusted so that the product of the combustor chamber pressure and the combustor diameter remained a constant. Exit nozzle sizes were chosen so that combustor velocity was approximately the same in all combustors. Inlet air temperature was held constant around 1000°R. Fuel/air ratios were selected at .025, .04, and .055. A spark plug, modified to burn hydrogen with air, was used as a pilot flame to ignite the fuel mixture in the chamber. The ignitor was used only to initiate the combustion and then was switched off. Lean blow-out limits, combustion efficiency, and combustor instability characteristics were obtained for each test condition. Rich blow-out limits were recorded when they occurred within the range of operating conditions. Photographs were taken of oscilloscope traces from an unbonded strain gauge pressure transducer located on the inlet so that the frequency and amplitude of any pressure oscillations could be determined. In addition to the base conditions, the pressure level within each of the combustors was varied by adjusting the air flow. Velocities within the combustor were varied by using different area exit nozzles.

Fig. 7 gives the combustion efficiency results for the baseline conditions. At low fuel/air ratios the product of pressure diameter, PD, held reasonably constant, and comparable combustion efficiencies were obtained, thus validating

the pressure scaling relationship. At higher fuel/air ratios, however, the performance of the smallest combustor (2" D) fell off markedly, possibly due to the relatively large heat loss. Performance for the 4" combustor consistently remained slightly higher than the 3" or 5" combustor, suggesting that some secondary effect such as a difference in tolerance on fuel injector size and location was responsible, rather than the scaling relationship itself.

Figs. 8. 9, and 10 show the results of all the test conditions attempted for fuel/air ratios of .025, .04, and .055, respectively. In these figures an indication of whether smooth combustion, combustion instability, or no combustion was encountered at a given chamber pressure and combustor entrance Mach number, M_3. The highest inlet Mach number data shown correspond to a choked constant area combustor without an exit nozzle. Combustion could not be sustained under those conditions for all cases attempted. Where combustion instability was encountered, the frequency and amplitude of the pressure oscillation divided by mean chamber pressure is also given.

Definite trends can be observed from the above figures. At the low fuel/air ratio, Fig. 8, combustion instability occurred in all 4 combustors when the smallest exit area nozzles ($A_*/A_3 < .2$) were used. This was a low frequency combustion instability of around 160 to 220 cycles/sec. with very large amplitude pressure oscillations. Good combustion was achieved in most cases for the design exit area nozzles ($A_*/A_3 \sim .5$), which corresponded to combustor velocities, V_3, of from 200 to 300 ft/sec. Combustion efficiencies were essentially constant except for the 2" and 3" chambers where combustion efficiency decreased when tested at the lower chamber pressures. Sustained combustion was not obtainable with the 2" chamber with the large area exit nozzle ($A_*/A_3 \sim .75$) or for any of the combustors when no exit nozzle was utilized ($A_*/A_3 = 1$).

As fuel/air ratio was increased to .04, Fig. 9, a higher frequency combustion instability occurred in the 2" chamber at the design nozzle area ratio. Combustion could not be sustained at other velocities or at low pressures for the 2" combustor. Likewise, combustion could not be sustained with the 3" combustor at the lower pressure conditions. At the highest fuel/air ratio tested, Fig. 10, the above trends continued with good combustion becoming more difficult to achieve for the smaller combustors (2" and 3" D).

The above results indicate that for the size range of combustors tested, pressure scaling is reasonably valid, except perhaps for the very small combustors where the percentage of heat loss becomes significant. This implies that small scale dump combustors should be tested at higher pressure levels in order to simulate the combustion process of full scale combustors at altitude conditions.

Combustor L/D

The 5" D combustor was tested with different length chambers varying from 7 1/2" to 30" in order to determine the L/D effect on dump combustor performance. Test conditions remained the same as during the base scale model tests. These results are shown in Fig. 11. A strong L/D effect is noted. A L/D of 6 was required in order to obtain combustion efficiencies of 90%. It should be stated that the combustion efficiencies given are for essentially cold wall combustors obtained directly from thrust measurements and are not corrected for heat loss. In previous tests conducted with an ablative lined chamber [5], combustion efficiency was observed to increase up to 10% with time as the ablative walls of the chamber heated up.

Fuel Additives

Shock tube studies [8, 9] have shown that relatively small amounts of n-propyl nitrate and ferrocene can effectively reduce the ignition delay times of Shelldyne fuel. Fuel blends consisting of Shelldyne-H and 7 1/2% by volume of n-propyl nitrate, toluene, and toluene-ferrocene were tested in the 5" D combustor. Toluene was included primarily to alter the physical properties of the blend and reduce viscosity. Fig. 17 shows this data for the base condition, a high L/D combustor, and a low temperature case. Results were disappointing in that combustion efficiencies were lower with all of the additives than those obtained with pure Shelldyne. Similar results were obtained when the propyl nitrate concentration was increased to 15%. This indicates that the dump burner used in this study is not chemical reaction rate limited.

Flame Stabilization

Blow-out data obtained from the previous tests using JP-4 fuels is shown in Fig. 18. Here the overall f/a ratio at which rich and lean blow-out occurred is plotted against a stability correlation parameter. With the exception of the runs with small nozzle area ratios ($A_*/A_3 < .2$), this correlation parameter appears to fit the data nicely considering that all four scale combustors are included. Also shown for comparative purposes are results for disk, cone, and hemisphere flameholders obtained at nearly the same inlet temperature [10]. The equivalent dimension, d_e, used for the dump combustor in this comparison, was $d_e = (D_3-D_2)/2$. It is noted that the lean blow-out limit for the dump combustors occurs at a much smaller f/a ratio than do the conventional flameholder combustors. It is thought that this is due to the relatively small amount of pre-mixing of the liquid spray which occurs upstream of the dump.

This would allow the local f/a ratio in the recirculation zone to be much higher, corresponding to the more classical pre-mixed lean blow-out limit.

Generalized Performance

Performance results obtained from all of the previous tests using JP-4 fuel were analyzed in an attempt to find a single parameter correlation. The range of variables included in this data are listed below:

Combustor Diameter, D_3	2 → 5"
Combustor L/D	1.5 → 6
Nozzle Area Ratio, A_*/A_3	.14 → .76
Dump Area Ratio, A_3/A_2	2.5 → 7.1
Inlet Velocity, V_2	330 → 1510 ft/sec
Combustor Velocity, V_3	80 → 440 ft/sec
Chamber Pressure, P_c	27 → 92 psia
Combustor Inlet Temperature, T_{T_2}	290 → 790°F
Fuel/Air Ratio, f/a	.025 → .055

Fig. 19 gives 9 different correlations that were applied to this data. These correlations were obtained either from ramjet combustion open literature [11], contractors usage, or modifications to previous correlations. In cases where an approach velocity was required, 2 computations were made using both the inlet duct velocity, V_2, and the combustor entrance velocity after the dump, V_3. Combustion efficiency was then plotted on semi-log paper against the various correlations. In most cases trends were not identifiable. Figs. 20 and 21 are examples of this in which η_c is plotted against a burner severity parameter, $W_A/A_* \ (T_{T_2}/1000)^2$, and a characteristic length correlation, $L(D_4/D^*)^2(T_{T_2}/1000)$. Fig. 22 shows similar results when η_c is plotted against

the stability parameter that was used for correlating the blow-out results shown in Fig. 18. Much better results are obtained when a modified version to the well-known Longwell parameter [12] is employed. These results are shown in Fig. 23. The assumption made in obtaining this correlation was that the reaction volume for the dump combustor was limited to the center core region as defined by the exit nozzle area.

Combustor Pressure Losses

Conventionally, ramjet burner pressure losses have been correlated by plotting the pressure ratio across the burner versus the sonic throat air specific stream thrust, S_{a*}, divided by the square root of the inlet total temperature, T_{T2}. This parameter has not been very successful in correlating pressure losses in dump combustors where the major losses are aerodynamic rather than thermodynamic. It was found [13] that the cold flow pressure losses of dump combustors could be correlated if the losses were plotted versus Mach number of the flow at the entrance to the combustor, M_2. The correlation took the form

$$P_{T_3}/P_{T_2} = e^{-\frac{\gamma}{2} N_D M_2^2}$$

where N_D was a function of the area ratio across the dump station, A_3/A_2.

Results obtained from this study have shown that even this correlation becomes unsatisfactory when combustion is occurring in the chamber. Contrary to the logical expectation that the losses would be somewhat greater due to combustion, it was found that the losses are less at the same inlet Mach number with combustion than without combustion. This reduced loss is apparently caused by the modification of the pressure in the recirculation zone by the combustion. Unpublished work here at the Air Force Aero Propulsion Lab has

shown that the pressure in the recirculation zone of the dump combustor is about 75% of the inlet static pressure for a combustor to inlet area ratio of 4 when no combustion is occurring. With efficient combustion occurring in the chamber, this pressure rises to a value essentially equal to the inlet static pressure. If it is postulated that the degree of pressure rise is related to the combustion efficiency, then pressure losses with combustion can be correlated by the following expression:

$$\psi = \frac{P_{T_4}}{P_{T_2}} \frac{A_3}{A_2} \left[1 + \gamma M_2^2 + \xi \, (A_3/A_2 - 1) \right]^{-1.06686}$$

where

$$\xi = (D_2/D_3)^{1/2} + [1-(D_2/D_3)^{1/2}] \, \eta_c$$

Details in obtaining these expressions are given in Appendix A.

The results of plotting this correlating parameter versus inlet duct Mach number are shown in Fig. 24. The majority of this data is from the 4" and 5" diameter combustion chambers and covers combustion efficiencies of from 29% to 90%. Also shown in Fig. 24 are some typical data taken from tests performed at The Marquardt Company on full scale hardware. This engine suffered additional losses due to flameholders in the inlet duct but the agreement with the present data is still quite good. Fig. 25 shows a comparison of the combustor pressure losses using this correlation parameter along with two previously used pressure loss correlations, namely N_D and C_{D_B} where

$$C_{D_B} = \frac{S_{a_3}' - S_{a_3}}{\frac{\gamma}{2} P_3' \quad A_3 (M_3')^2}$$

and the primes are fictitious conditions obtained by isentropic expansion from A_2 to A_3. Large differences between these three methods are evident at the higher inlet Mach numbers.

SECTION IV

CONCLUSIONS

Pressure scaling may be applied (with caution) to dump combustors.

Combustion instability can occur in dump combustors, particularly in combustors with small nozzle area ratios.

Combustor L/D is an important parameter in dump combustors which do not contain flameholders. $L/D \geq 4.5$ is required to obtain good combustion efficiency.

Combustion efficiency is dependent upon inlet air temperatures in the range of from 300 to 800°F.

Shelldyne fuel is particularly sensitive to low inlet air temperatures. At 290°F the combustion efficiency for Shelldyne-H decreases drastically with increasing fuel/air ratio when compared to JP-4 results.

Fuel additives of n-propyl nitrate, toluene, and ferrocene did not improve combustion efficiency when added to Shelldyne.

Currently used single parameter correlations do not adequately correlate combustor efficiency results when applied over a wide range of combustor configurations and test conditions. The best results were obtained when a modified version of the Longwell parameter was used.

Pressure losses covering a wide range of geometrical variables and engine conditions are satisfactorily correlated by a single variable derivable from one dimensional relations requiring only one experimentally determined function, ξ.

SECTION V

REFERENCES

1. Lefebvre, A. H. and Halls, G. A., "Some Experiences in Combustion Scaling", AGARD Colloquium: Advanced Aero Engine Testing, Pergamon Press, 1959.
2. Stewart, D. G. and Quigg, G. C., "Similarity and Scale Effect in Ramjet Combustors", Ninth Symposium (International) on Combustion, pp 907-921, Academic Press, 1963.
3. Hojnacki, J. T., "Ramjet Engine Fuel Injection Studies", AFAPL-TR-72-76, August 1972.
4. McBride, B. and Gordon, S., "ICRPG, One Dimensional Equilibrium Reference Program", May, 1968, NASA-Lewis Research Center.
5. Hojnacki, J. T. and Schwartzkopf, K. G., "Recent Dump Combustor Developments", CPIA Publication 231, Vol. II, 9th JANNAF Combustion Meeting, September 1972.
6. Ortwerth, P. J., Hojnacki, J. T., and Barclay, L. P., "Liquid Ramjet Dump Combustor Development", CPIA Publication 219, Vol. III, 1971 JANNAF Combined Propulsion Meeting, November 1971.
7. Ingebo, R. and Foster, H., "Drop Size Distribution for Cross-Current Breakup of Liquid Jets", NACA TN-4087, October 1957.
8. Siminski, V. J. and Wright, F. J. (Vol. 1); Edelman, R., Economos, C., and Fortune, O. (Vol. 2), "Research on Methods of Improving the Combustion Characteristics of Liquid Hydrocarbon Fuels", AFAPL-TR-72-24, February 1972.

9. McCarty, M., Jr., Maycock, J. M., and Skean, D., "A Shocktube Study of the Combustion of Shelldyne-H with Additives", RIAS Division of Martin Marietta Corporation.

10. Ozawa, R. I., "Survey of Basic Data on Flame Stabilization and Propagation for High Speed Combustion Systems", AFAPL-TR-70-81, January 1971.

11. Dugger, G. L./Editor, "Ramjets", AIAA Selected Reprints, Vol. VI, June 1969.

12. Longwell, J. P., "Combustion Problems in Ramjets", Fifth Symposium (International) on Combustion, pp 48-56, Reinhold Publishing Corporation, New York, 1955.

13. Barclay, L. P., "Pressure Losses in Dump Combustors", AFAPL-TR-72-57, October 1972.

SECTION VI

APPENDIX A

DERIVATION OF PRESSURE LOSS CORRELATION PARAMETER

If one assumes the static pressure in the recirculation zone is some fraction, ξ, of the inlet static pressure, an expression can easily be derived for the total pressure loss across the dump region by making use of the X, Y and Z Mach number functions, where

$$X = \frac{\sqrt{\gamma}\, M}{\left[1+\frac{\gamma-1}{2} M^2\right]^{\frac{\gamma+1}{2(\gamma-1)}}}$$

$$Y = \frac{M\sqrt{\gamma(1+\frac{\gamma-1}{2}M^2)}}{1+\gamma M^2}$$

$$Z = X/Y$$

The one-dimensional weight flow and stream thrust equations then become

$$\dot{W} = P_T\ A\ X\ \sqrt{gM/\mathcal{R}T_T}$$

and

$$F = \frac{\dot{W}}{g} V+PA = P_T\ A\ Z$$

One then finds from the one-dimensional momentum equation, that for a constant pressure in the recirculation zone

$$Y_3 = \frac{Y_2(1+\gamma M_2{}^2)}{[1+\gamma M_2{}^2+\xi(A_3/A_2-1)]}$$

and

$$\frac{P_{T_3}}{P_{T_2}} = \frac{X_2 A_2}{X_3 A_3}$$

For small Mach numbers in the combustor, the functions X_3 and Y_3 can be expressed as

$$X_3 = B\ M_3{}^C$$

$$Y_3 = D\ M_3{}^E$$

One can then write an expression for P_{T3}/P_{T2} in terms of M_2, A_3/A_2 and ξ.

$$\frac{P_{T3}}{P_{T2}} = \frac{X_2}{1.13}\frac{A_2}{A_3}\left[\frac{Y_2(1+\gamma M_2^2)}{\{1+\gamma M_2^2+\xi(A_3/A_2-1)\}}\right]^{-1.06686}$$

The function ξ should be a function of the combustion efficiency, η_c, as well as the area ratio of the burner to the inlet. The proposed variation is

$$\xi = (D_2/D_3)^{1/2} + [1-(D_2/D_3)^{1/2}]\,\eta_c$$

One then expects the correlation parameter

$$\psi = \frac{P_{T3}}{P_{T2}}\frac{A_3}{A_2}\quad\{1+\gamma M_2^2+\xi(A_3/A_2-1)\}^{-1.06686}$$

to be a function of the inlet Mach number and γ only and have a value

$$\psi = \frac{X_2}{1.13}\quad[Y_2(1+\gamma M_2^2)]^{-1.06686}$$

Since the pressure loss correlation parameter is based on one-dimensional relations one must obtain mean inlet and combustor total pressures to test the correlation. The most consistent results are obtained when these mean pressures yield the correct mass flows from the one-dimensional equations.

With the inlet flow to the combustor being subsonic one expects the static pressure across the inlet to be fairly uniform even if the total pressure is not uniform. Hence, by measuring the inlet static pressure, total temperature and mass flow, an average inlet Mach number from the mass flow equations can easily be determined:

$$\dot{W}_a = \frac{\sqrt{\gamma}\ M_2(1+\frac{\gamma-1}{2}M_2^2)^{1/2}\ P_2A_2\sqrt{Mg/\mathcal{R}}}{\sqrt{T_{T2}}}$$

Isentropic relations are then used to obtain a mean total pressure, P_{T2}, from M_2 and P_2.

The mean total pressure after combustion is calculated from the mean combustion temperature which was previously deduced from the thrust measurement. Here again use is made of the NASA thermochemical program to obtain the proper corrections for ideal, chemically reacting flows. The weight flow through a sonic nozzle is simply related to the area of the throat, A_*, the total pressure, P_{T4}, and the total temperature, T_{T4}, by the expression

$$\dot{W}_T = K_W \, P_{T4} \, A_* / \sqrt{T_{T4}}$$

where K_W is a function of the molecular weight, $\mathbf{M}$, and ratio of specific heats, γ, of the combustion products.

Values of K_W for RJ-5 and JP-4 are shown in Fig. 26. K_W is somewhat pressure sensitive at high temperatures and is stored in the data reduction program as a two-dimensional array with T_{T4} and P_{T4} as the independent variables.

With the measured total weight flow through the combustor, it is now a simple matter to compute a mean combustor total pressure which is consistent with the mass flow and the thrust of the combustor.

SECTION VII

APPENDIX B

TABULATION OF JP-4 AND RJ-5 COMBUSTION EFFICIENCY DATA

Preceding page blank

Dump Combustor Data
JP-4

(*) could not sustain combustion

Test	D_3 (inches)	D_2	L (inches)	D*	f/a	$\dot{W}a$ (#/sec)	T_{02} (°R)	P_3 (psia)	η_c
5" base	5	2.5	15	3.5	.027	3.89	990	36.72	.623
5" base	5	2.5	15	3.5	.039	3.37	991	35.46	.618
5" base	5	2.5	15	3.5	.054	3.01	993	37.75	.749
High P	5	2.5	15	3.5	.027	6.21	991	59.32	.649
High P	5	2.5	15	3.5	.040	5.84	995	64.19	.686
High P	5	2.5	15	3.5	.054	5.25	997	64.16	.696
High P	5	2.5	15	3.5	.055	5.80	1025	75.03	.798
Low V	5	2.5	15	2.0	.026	1.32	1001	38.12	.654
Low V	5	2.5	15	2.0	.037	1.16	1013	36.94	.643
Low V	5	2.5	15	2.0	.050	1.05	1028	35.11	.552
High V	5	2.5	15	4.25	.025	5.59	1033	35.91	.639
High V	5	2.5	15	4.25	.038	5.00	1016	36.85	.648
High V	5	2.5	15	4.25	.053	4.43	992	34.39	.542
High V	5	2.5	15	5.0	.025	7.35	990	*	*
High V	5	2.5	15	5.0	.040	6.13	990	*	*
High V	5	2.5	15	5.0	.055	5.43	990	*	*
4" base	4	2.0	12	2.75	.025	2.95	1026	46.13	.714
4" base	4	2.0	12	2.75	.040	2.59	1017	49.40	.836
4" base	4	2.0	12	2.75	.055	2.30	997	48.29	.812
Low P	4	2.0	12	2.75	.024	2.48	1009	37.00	.637
Low P	4	2.0	12	2.75	.038	2.12	1002	38.41	.765
Low P	4	2.0	12	2.75	.054	1.86	998	37.92	.759
High P	4	2.0	12	2.75	.025	4.18	1011	64.30	.681
High P	4	2.0	12	2.75	.038	3.58	997	67.01	.843
High P	4	2.0	12	2.75	.052	3.25	1008	67.89	.833

Preceding page blank

Dump Combustor Data
JP-4

(*) could not sustain combustion

Test	D_3 (inches)	D_2	L (inches)	D*	f/a	$\dot{W}a$ (#/sec)	T_{02} (°R)	P_3 (psia)	η_c
High P	4	2	12	2.75	.024	6.08	1011	92.05	.671
High P	4	2	12	2.75	.040	5.09	1014	97.13	.838
High P	4	2	12	2.75	.055	4.58	1017	96.24	.810
Low V	4	2	12	1.75	.026	1.23	1008	46.31	.645
Low V	4	2	12	1.75	.039	1.15	1000	50.75	.746
Low V	4	2	12	1.75	.054	1.01	1000	47.74	.667
High V	4	2	12	3.5	.024	4.08	1006	45.62	.676
High V	4	2	12	3.5	.039	4.05	981	46.01	.708
High V	4	2	12	3.5	.055	3.56	980	*	*
High V	4	2	12	4.0	.025	5.88	1000	*	*
High V	4	2	12	4.0	.040	4.90	1000	*	*
High V	4	2	12	4.0	.055	4.34	1000	*	*
3" base	3	1.5	9	2.0	.026	2.10	1029	60.44	.623
3" base	3	1.5	9	2.0	.042	1.81	1031	63.87	.749
3" base	3	1.5	9	2.0	.055	1.65	1029	62.88	.725
Low P	3	1.5	9	2.0	.025	1.63	1041	47.38	.667
Low P	3	1.5	9	2.0	.040	1.38	1045	*	*
Low P	3	1.5	9	2.0	.055	1.20	1045	*	*
High P	3	1.5	9	2.0	.025	3.19	1010	90.72	.630
High P	3	1.5	9	2.0	.039	2.79	1003	96.54	.771
High P	3	1.5	9	2.0	.054	2.43	1025	93.76	.761
Low V	3	1.5	9	1.25	.027	.88	1029	67.35	.700
Low V	3	1.5	9	1.25	.039	.79	1034	65.96	.655
Low V	3	1.5	9	1.25	.055	.65	1035	*	*

Dump Combustor Data
JP-4
(*) could not sustain combustion
(**) combustion instability too severe

Test	D_3 (inches)	D_2	L (inches)	D*	f/a	$\dot{W}a$ (#/sec)	T_{02} (°R)	P_3 (psia)	η_c
High V	3	1.5	9	2.5	.024	3.38	1024	59.51	.563
High V	3	1.5	9	2.5	.038	2.89	1023	63.32	.709
High V	3	1.5	9	2.5	.055	2.45	1020	*	*
High V	3	1.5	9	3.0	.025	4.41	1000	*	*
High V	3	1.5	9	3.0	.040	3.67	1000	*	*
High V	3	1.5	9	3.0	.055	3.25	1000	*	*
2" base	2	1	6	1.375	.023	1.59	1007	93.29	.626
2" base	2	1	6	1.375	.038	1.33	1026	91.79	.652
2" base	2	1	6	1.375	.052	1.23	1027	89.69	.560
Low P	2	1	6	1.375	.024	1.10	1010	63.85	.573
Low P	2	1	6	1.375	.041	.96	1015	67.57	.642
Low P	2	1	6	1.375	.055	.80	1015	*	*
Low P	2	1	6	1.375	.023	.60	1000	33.37	.509
Low P	2	1	6	1.375	.030	.60	994	31.91	.315
Low P	2	1	6	1.375	.04	.51	990	*	*
Low V	2	1	6	.75	.021	.68	1019	**	**
Low V	2	1	6	.75	.026	.57	1007	**	**
Low V	2	1	6	.75	.04	.50	1005	*	*
High V	2	1	6	1.75	.025	2.37	1000	*	*
High V	2	1	6	1.75	.04	2.00	1000	*	*
High V	2	1	6	1.75	.055	1.78	1000	*	*
High V	2	1	6	2.0	.025	2.94	1000	*	*
High V	2	1	6	2.0	.04	2.45	1000	*	*
High V	2	1	6	2.0	.055	2.17	1000	*	*

Dump Combustor Data
JP-4

(*) could not sustain combustion

Test	D_3 (inches)	D_2	L (inches)	D*	f/a	$\dot{W}a$ (#/sec)	T_{02} (°R)	P_3 (psia)	η_c
L/D	5	2.5	7.5	3.5	.026	3.86	1007	27.47	.151
L/D	5	2.5	7.5	3.5	.04	3.32	1005	*	*
L/D	5	2.5	7.5	3.5	.055	2.97	1005	*	*
L/D	5	2.5	11.25	3.5	.0250	3.84	1014	34.94	.580
L/D	5	2.5	11.25	3.5	.04	3.32	1028	32.43	.459
L/D	5	2.5	11.25	3.5	.055	2.95	1028	35.38	.645
L/D	5	2.5	22.5	3.5	.025	3.87	1001	38.70	.814
L/D	5	2.5	22.5	3.5	.04	3.32	1006	40.19	.903
L/D	5	2.5	22.5	3.5	.054	3.02	1009	39.42	.831
L/D	5	2.5	30	3.5	.025	3.89	996	39.99	.891
L/D	5	2.5	30	3.5	.04	3.33	1002	40.49	.915
L/D	5	2.5	30	3.5	.055	2.98	1005	39.64	.864
L*	5	2.5	7.5	2.0	.04	1.36	998	42.70	.573
L*	5	2.5	7.5	2.0	.039	1.17	993	35.65	.532
L*	5	2.5	7.5	2.0	.053	1.06	989	32.87	.410
L*	5	2.5	33.75	4.25	.025	5.58	1007	38.82	.829
L*	5	2.5	33.75	4.25	.039	4.81	1014	40.23	.893
L*	5	2.5	33.75	4.25	.054	4.29	1001	40.76	.910
T_{02}	5	2.5	15	3.5	.025	3.87	758	33.40	.588
T_{02}	5	2.5	15	3.5	.039	3.33	761	31.90	.523
T_{02}	5	2.5	15	3.5	.054	2.98	770	33.88	.615
T_{02}	5	2.5	15	3.5	.024	3.95	1245	39.17	.709
T_{02}	5	2.5	15	3.5	.039	3.37	1249	38.22	.698
T_{02}	5	2.5	15	3.5	.054	3.04	1243	39.41	.767

Dump Combustor Data
JP-4

Test	D_3 (inches)	D_2	L (inches)	D^*	f/a	$\dot{W}a$ (#/sec)	T_{02} (°R)	P_3 (psia)	η_c
A_3/A_2	4	1.5	12	2.71	.0263	2.93	1042	46.63	.644
A_3/A_2	4	1.5	12	2.71	.034	2.76	1045	48.03	.672
A_3/A_2	4	1.5	12	2.71	.423	2.49	1047	45.92	.650
A_3/A_2	4	1.5	12	2.71	.0481	2.36	1049	44.60	.628
A_3/A_2	4	1.5	12	2.71	.0566	2.28	1049	48.43	.732
A_3/A_2	4	2.5	12	2.71	.0241	3.13	1004	49.51	.708
A_3/A_2	4	2.5	12	2.71	.0315	2.86	1011	49.30	.716
A_3/A_2	4	2.5	12	2.71	.0395	2.70	1014	49.79	.707
A_3/A_2	4	2.5	12	2.71	.0474	2.45	1020	47.03	.673
A_3/A_2	4	2.5	12	2.71	.0532	2.57	1025	51.10	.655
L/D	4	2.0	9	2.75	.024	3.06	1002	43.36	.525
L/D	4	2.0	9	2.75	.039	2.58	997	40.96	.489
L/D	4	2.0	9	2.75	.054	2.33	999	46.12	.699
L/D	4	2.0	21	2.75	.025	3.04	1014	48.59	.775
L/D	4	2.0	21	2.75	.04	2.56	1027	49.45	.864
L/D	4	2.0	21	2.75	.054	2.32	1031	49.56	.854
8 inj.	4	2	12	2.75	.025	2.95	1026	46.13	.714
8 inj.	4	2	12	2.75	.032	2.72	1026	44.70	.657
8 inj.	4	2	12	2.75	.04	2.59	1017	49.40	.836
8 inj.	4	2	12	2.75	.047	2.39	1007	48.01	.839
8 inj.	4	2	12	2.75	.055	2.30	997	48.29	.812
4 inj.	4	2	12	2.75	.024	2.99	1016	46.02	.709
4 inj.	4	2	12	2.75	.032	2.73	1026	44.83	.655
4 inj.	4	2	12	2.75	.039	2.60	999	44.73	.636
4 inj.	4	2	12	2.75	.047	2.40	1010	45.92	.731
4 inj.	4	2	12	2.75	.054	2.33	1022	47.62	.759

Dump Combustor Data
RJ-5

Test	D_3 (inches)	D_2	L (inches)	D*	f/a	$\dot{W}a$ (#/sec)	T_{02} (°R)	P_3 (psia)	η_c
5" base	5	2.5	15	3.5	.028	3.78	1002	36.55	.680
5" base	5	2.5	15	3.5	.034	3.55	971	36.13	.673
5" base	5	2.5	15	3.5	.04	3.35	977	35.78	.664
5" base	5	2.5	15	3.5	.047	3.22	990	36.40	.666
5" base	5	2.5	15	3.5	.053	3.03	993	37.16	.744
High P	5	2.5	15	3.5	.028	6.63	1022	66.78	.770
High P	5	2.5	15	3.5	.042	5.72	1034	66.00	.779
High P	5	2.5	15	3.5	.058	5.07	1035	67.37	.839
L/D	5	2.5	30	3.5	.0272	3.94	981	36.1	.884
L/D	5	2.5	30	3.5	.0341	3.55	985	35.0	.886
L/D	5	2.5	30	3.5	.0415	3.34	989	36.1	.896
L/D	5	2.5	30	3.5	.0477	3.18	994	35.9	.887
L/D	5	2.5	30	3.5	.0552	2.99	998	35.1	.884
Low T_{02}	5	2.5	15	3.5	.028	3.87	753	33.97	.583
Low T_{02}	5	2.5	15	3.5	.035	3.51	753	31.82	.515
Low T_{02}	5	2.5	15	3.5	.041	3.27	745	30.06	.463
Low T_{02}	5	2.5	15	3.5	.047	3.11	750	29.21	.429
Low T_{02}	5	2.5	15	3.5	.054	2.94	766	27.79	.376
High T_{02}	5	2.5	15	3.5	.0276	3.91	1244	31.5	.729
High T_{02}	5	2.5	15	3.5	.0333	3.65	1236	31.8	.682
High T_{02}	5	2.5	15	3.5	.0413	3.34	1229	32.0	.677
High T_{02}	5	2.5	15	3.5	.0471	3.20	1223	32.6	.691
High T_{02}	5	2.5	15	3.5	.054	3.04	1220	32.3	.662
4 inj.	5	2.5	15	3.5	.028	3.91	972	36.78	.631
4 inj.	5	2.5	15	3.5	.041	3.35	981	35.94	.656
4 inj.	5	2.5	15	3.5	.054	3.04	994	34.79	.599

- "Pressure Scaling"

$PL = CONST$
$V = CONST$
$T_{IN} = CONST$
$f/a = CONST$
Geometric Similarity

1. Reynolds Nr. - Affects Speed of Mixing
   $Re \alpha PVL$
2. Damköhler 1st - Fixes Residence Time in Relation to Reaction Time

$$D_1 = \frac{L}{\tau V} \alpha \frac{p^{n-1}L}{V}$$

For n = 2
(Apparent Reaction Order of 2)

$$\left.\begin{array}{l} Re \rightarrow PL(V) \\ D_1 \rightarrow \frac{PL}{V} \end{array}\right\} \quad \begin{array}{l} PL = CONST \\ V = CONST \end{array}$$

- Major Difficulties

1. Fuel Distribution Process Causes Scaling Difficulties When Penetration is a Factor. (Both Diffusion and Penetration Similarity Required).
2. Mfg. of Scale Models is Difficult Due To Accuracy Required to Insure Exact Geometric Similarity.

- Second Order Effects

1. Heat Transfer Effects on Wall Temperature.
2. Helmholtz Resonator Effects on Combustion Instability.

Figure 1. Combustor Scaling Relationships

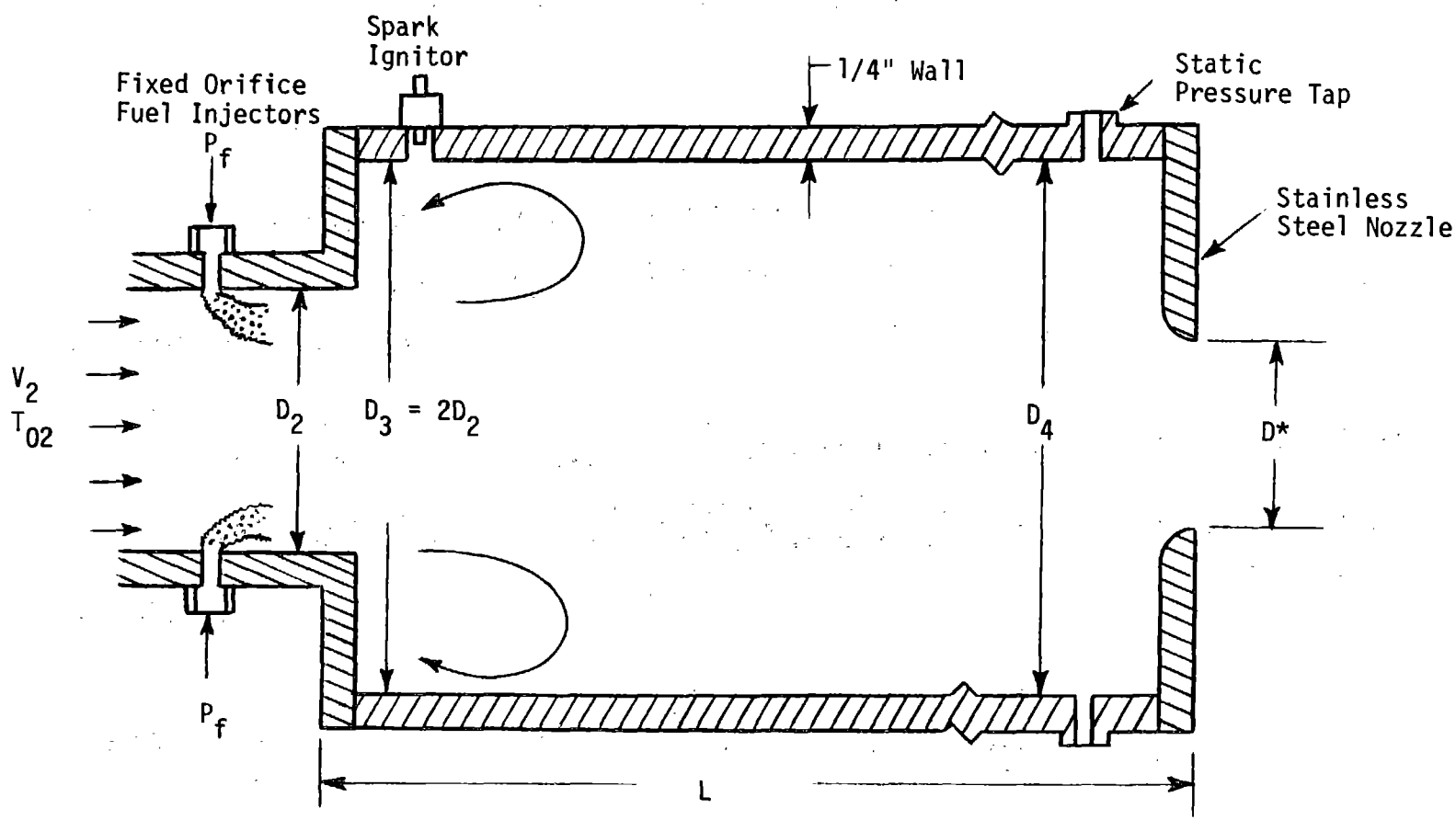

Figure 2. Sketch of Test Hardware

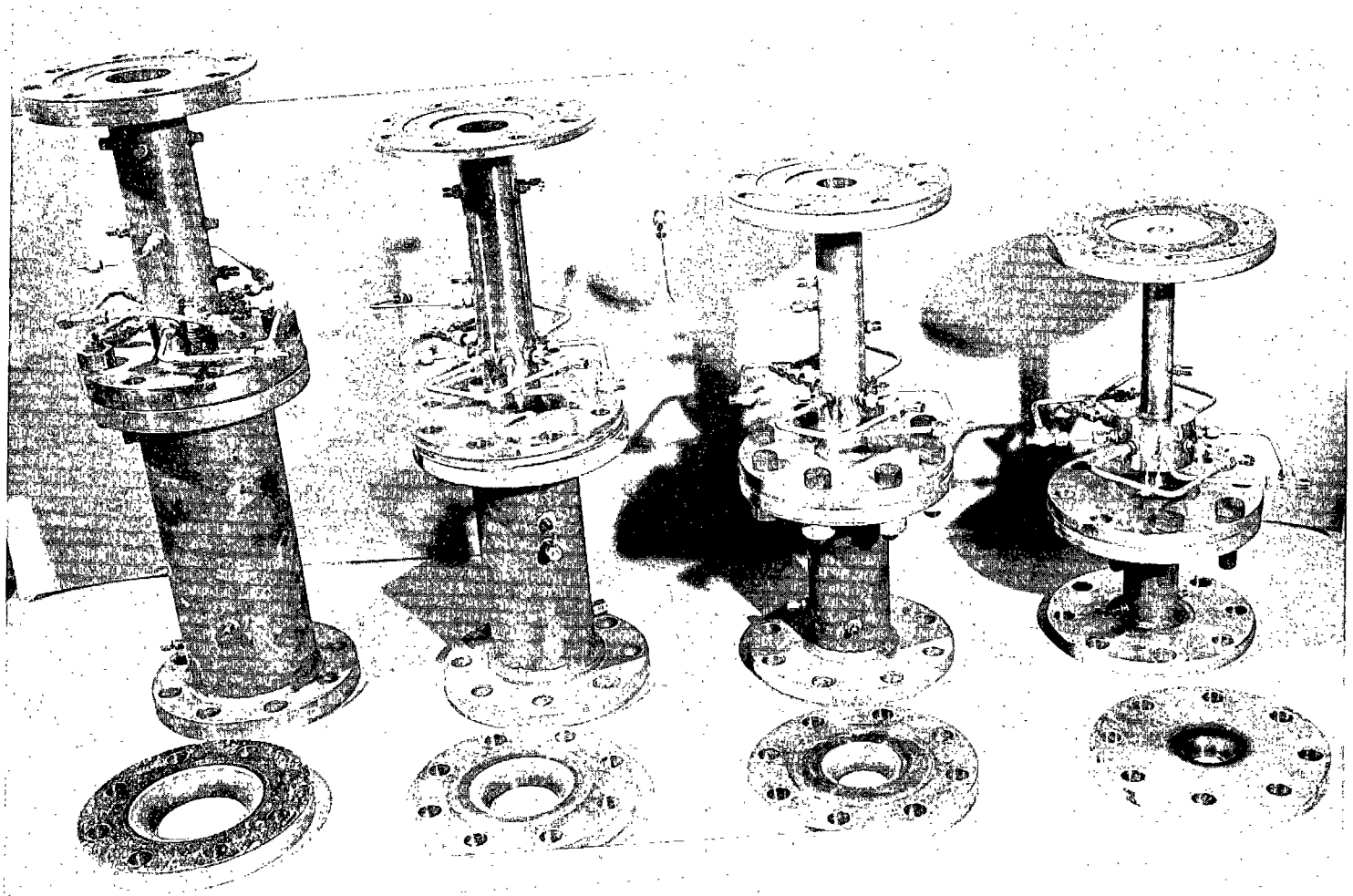

Figure 3. Scale Model Combustors

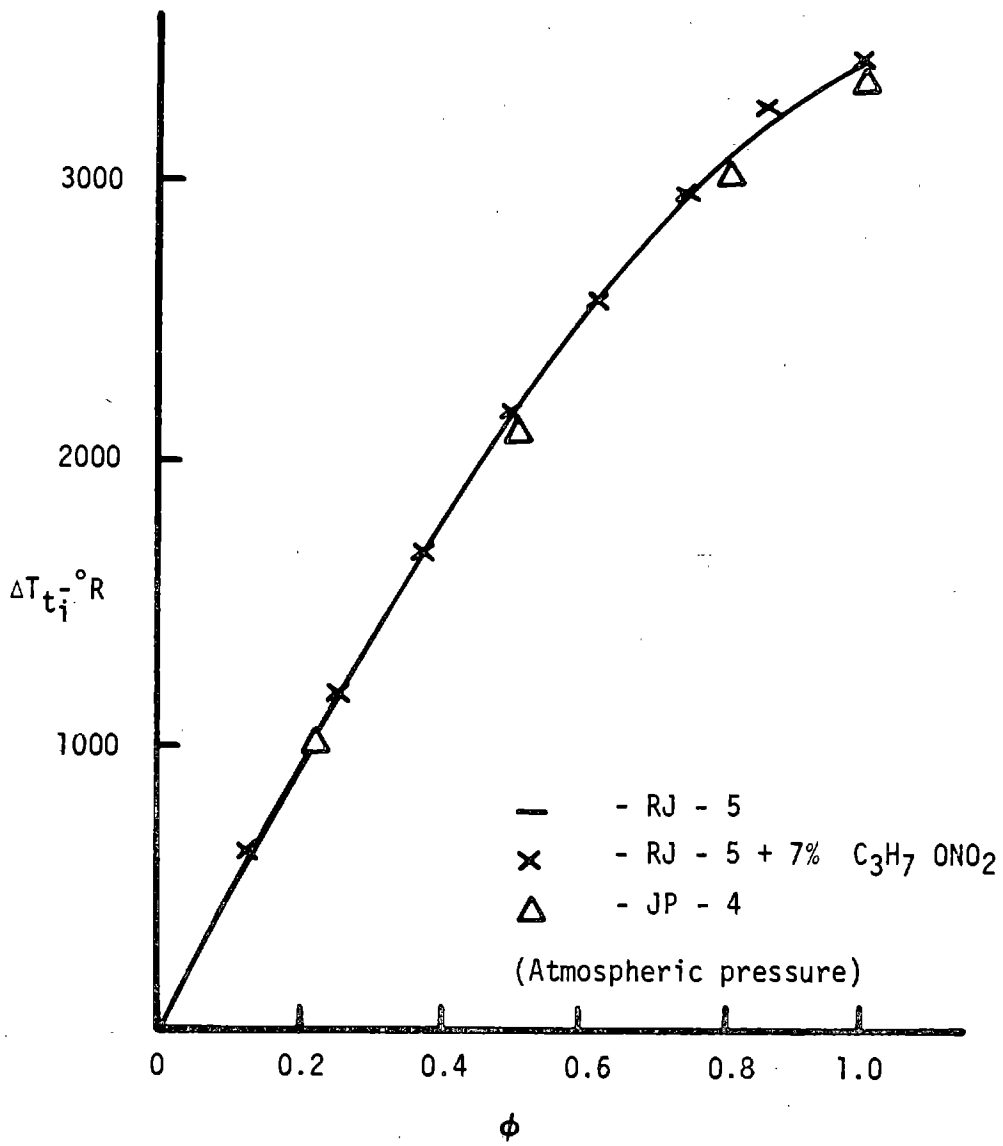

Figure 4. Ideal Temperature Rise

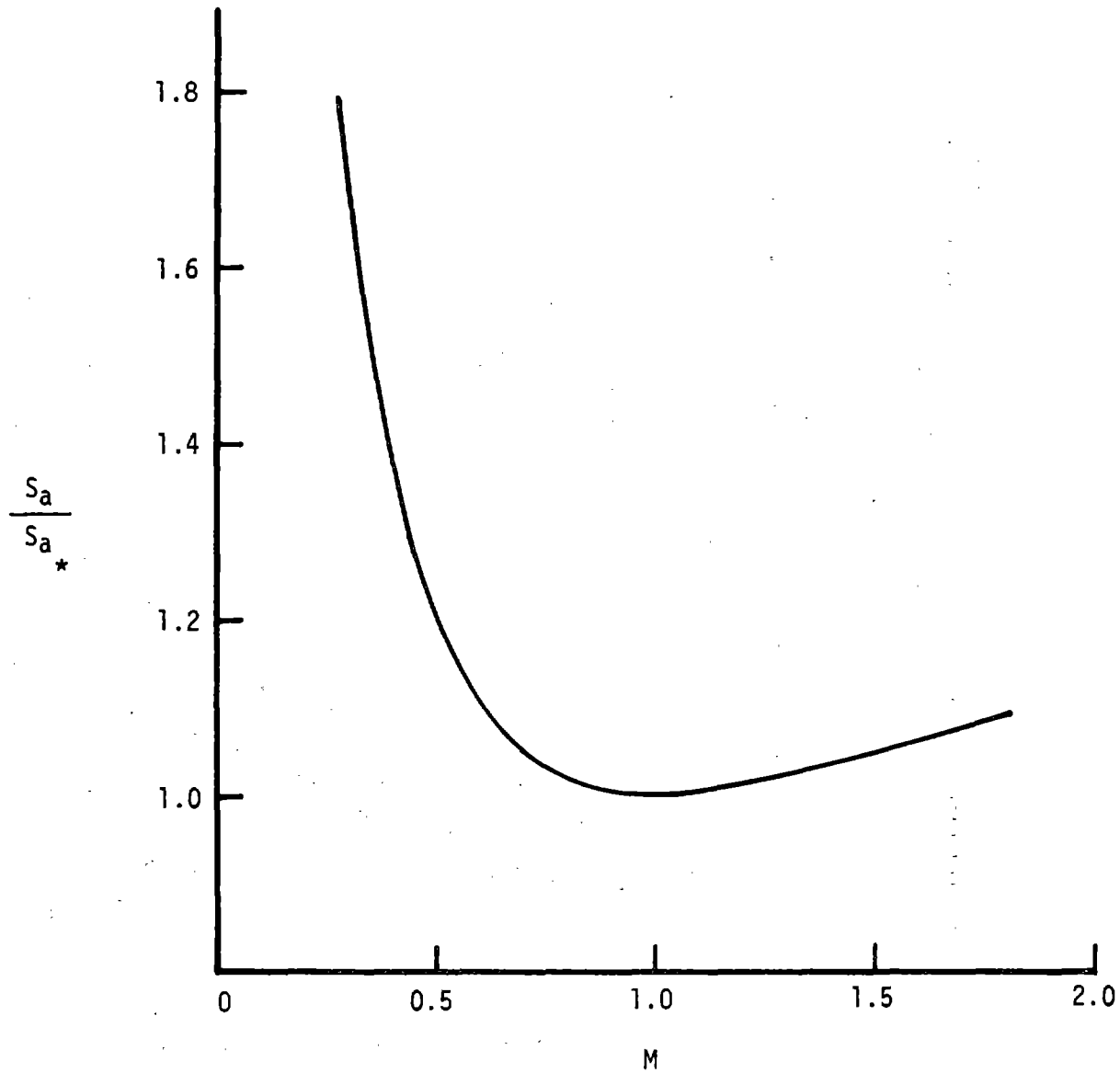

Figure 5. Air Specific Stream Thrust

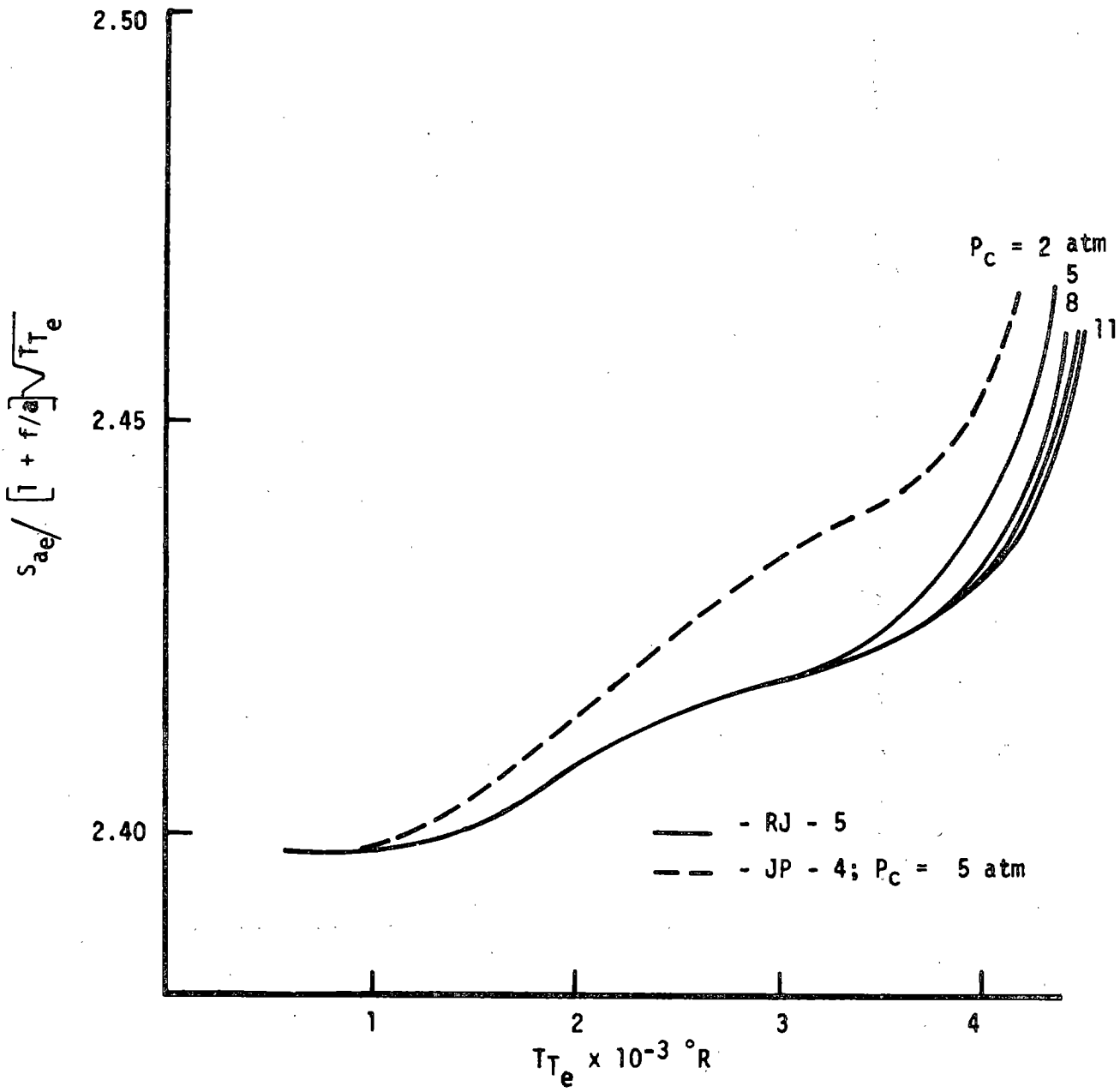

Figure 6. Air Specific Stream Thrust for Combustion Gases

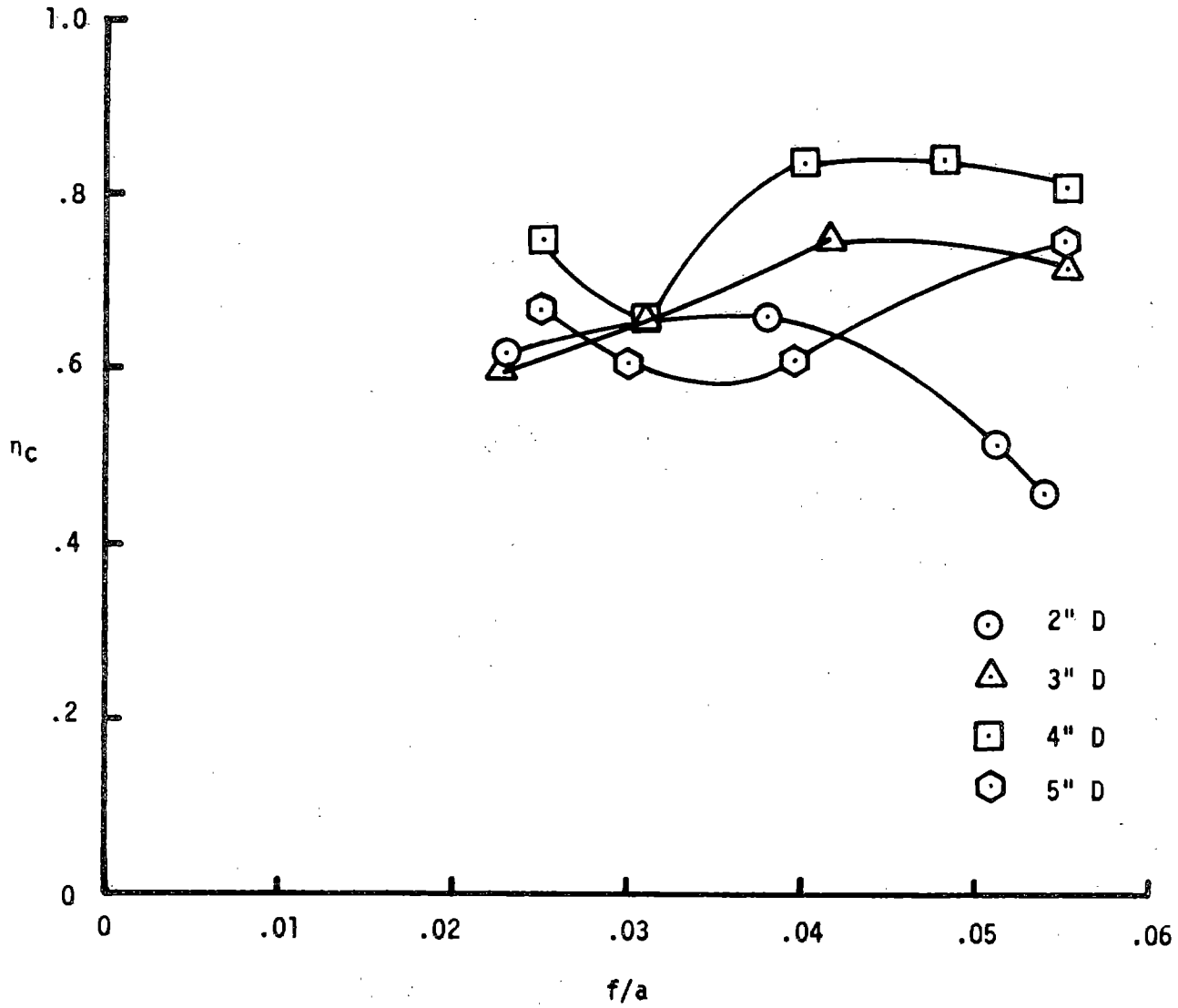

Figure 7. Pressure Scaling Tests

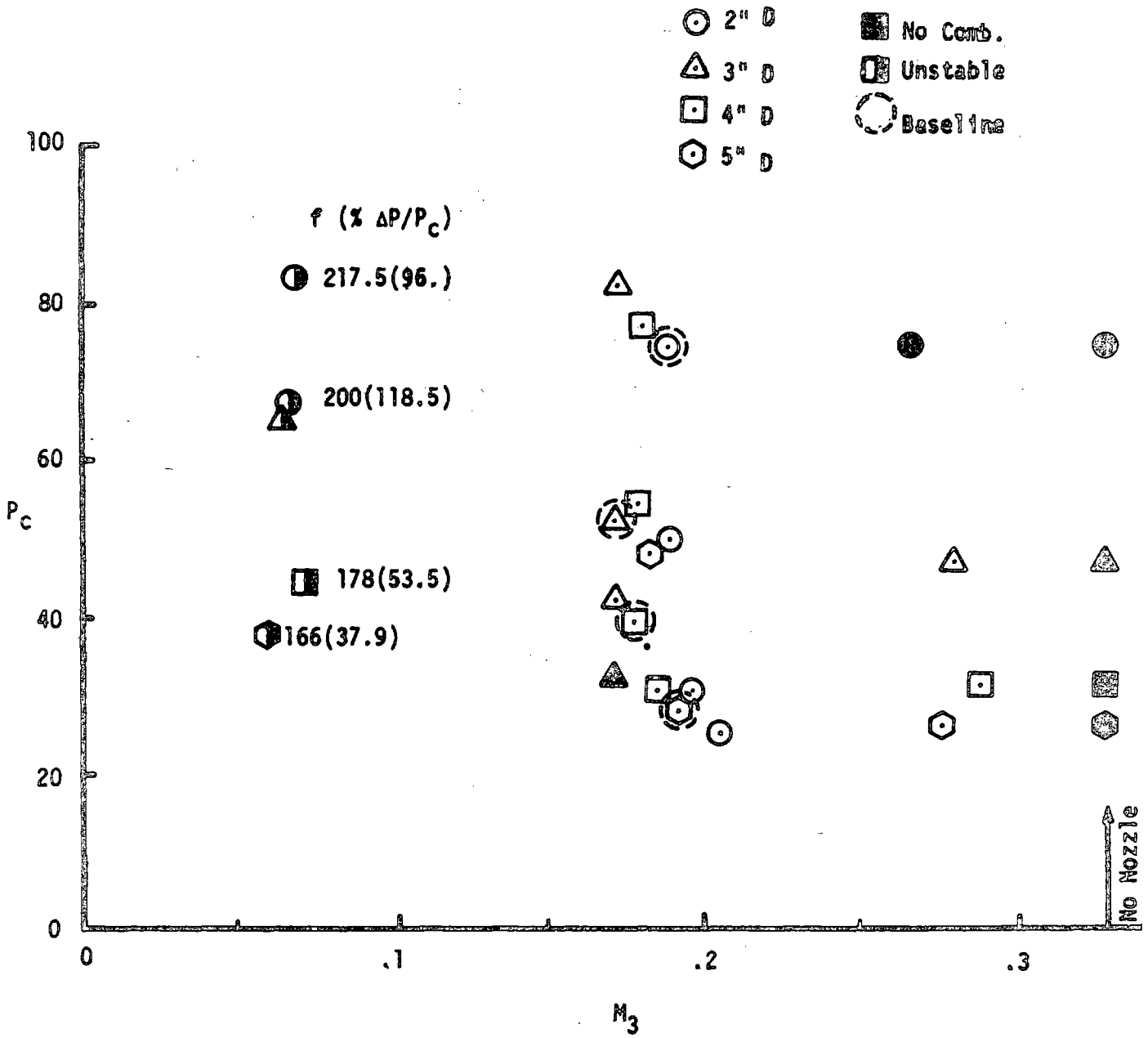

Figure 8. Scale Model Test f/a = .025

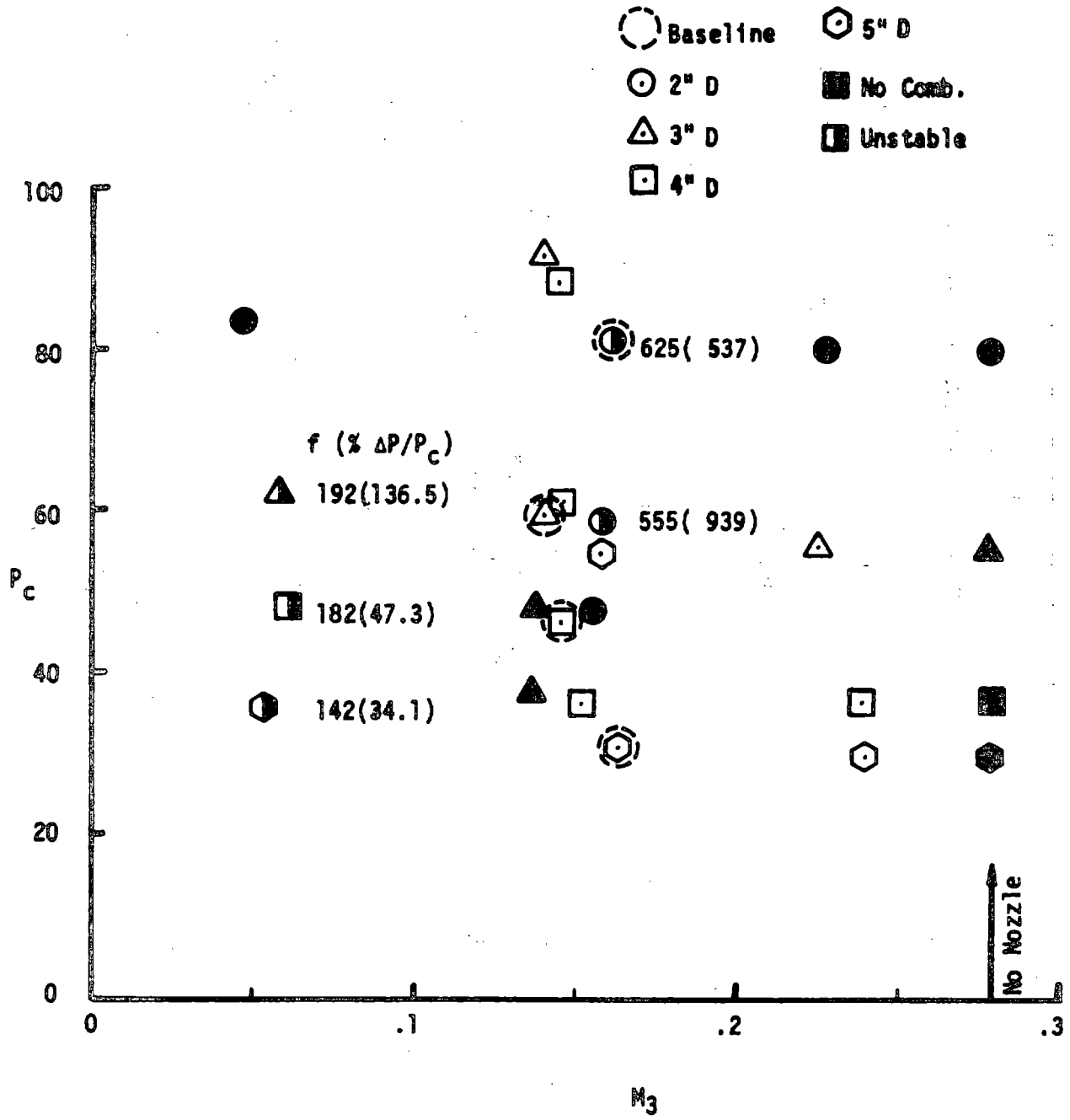

Figure 9. Scale Model Test f/a = .040

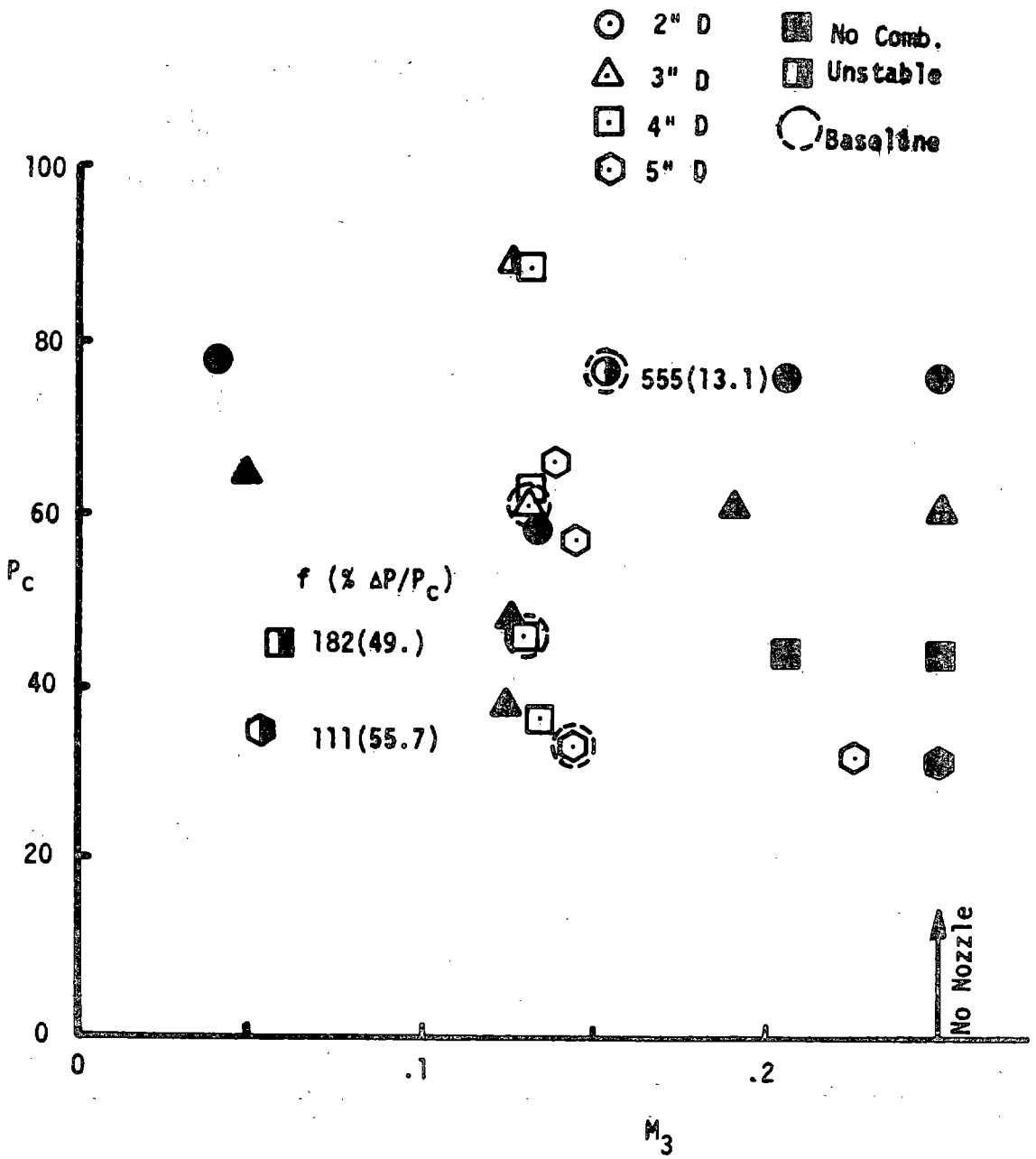

Figure 10. Scale Model Test f/a = .055

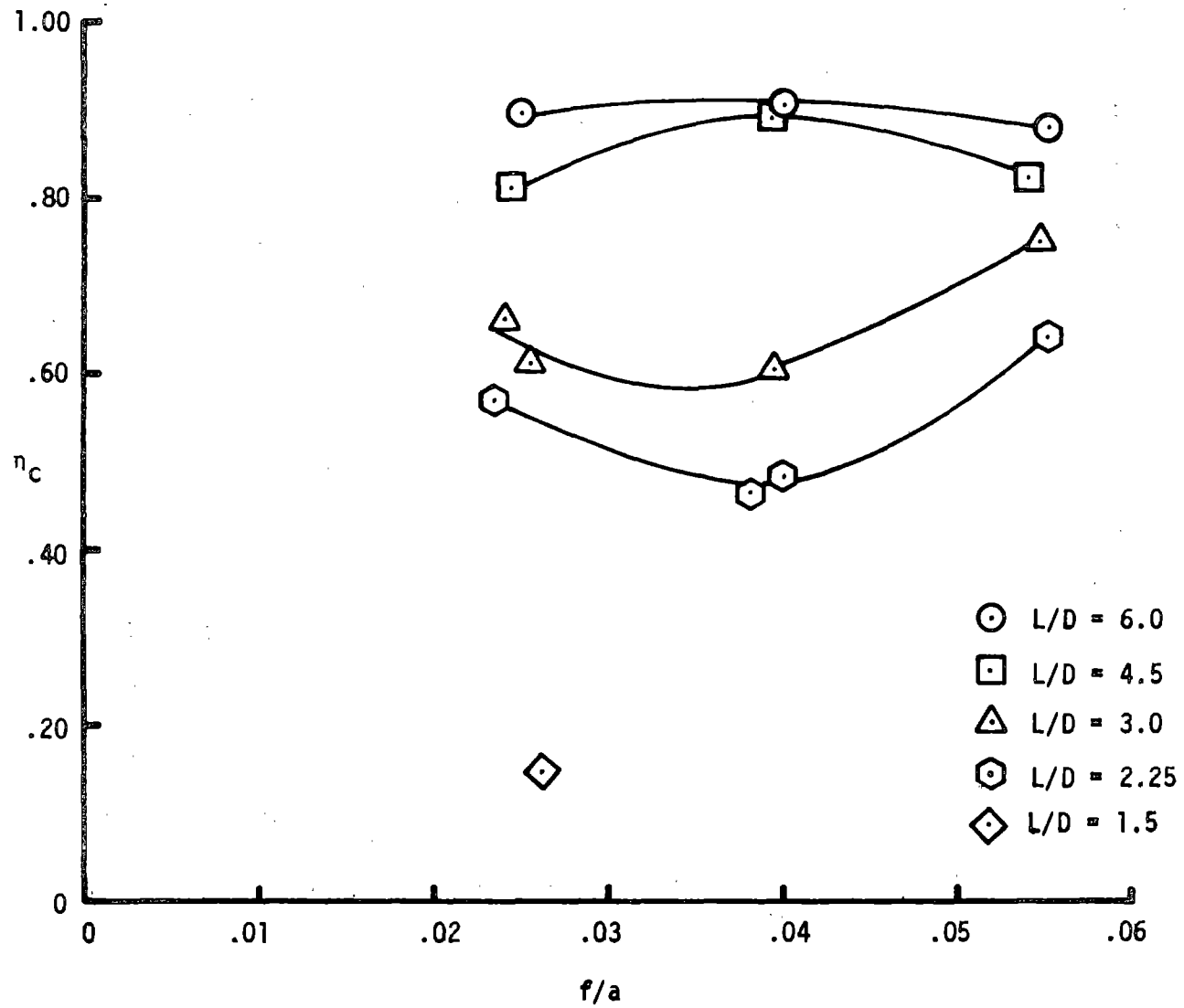

Figure 11. Effects of Combustor L/D

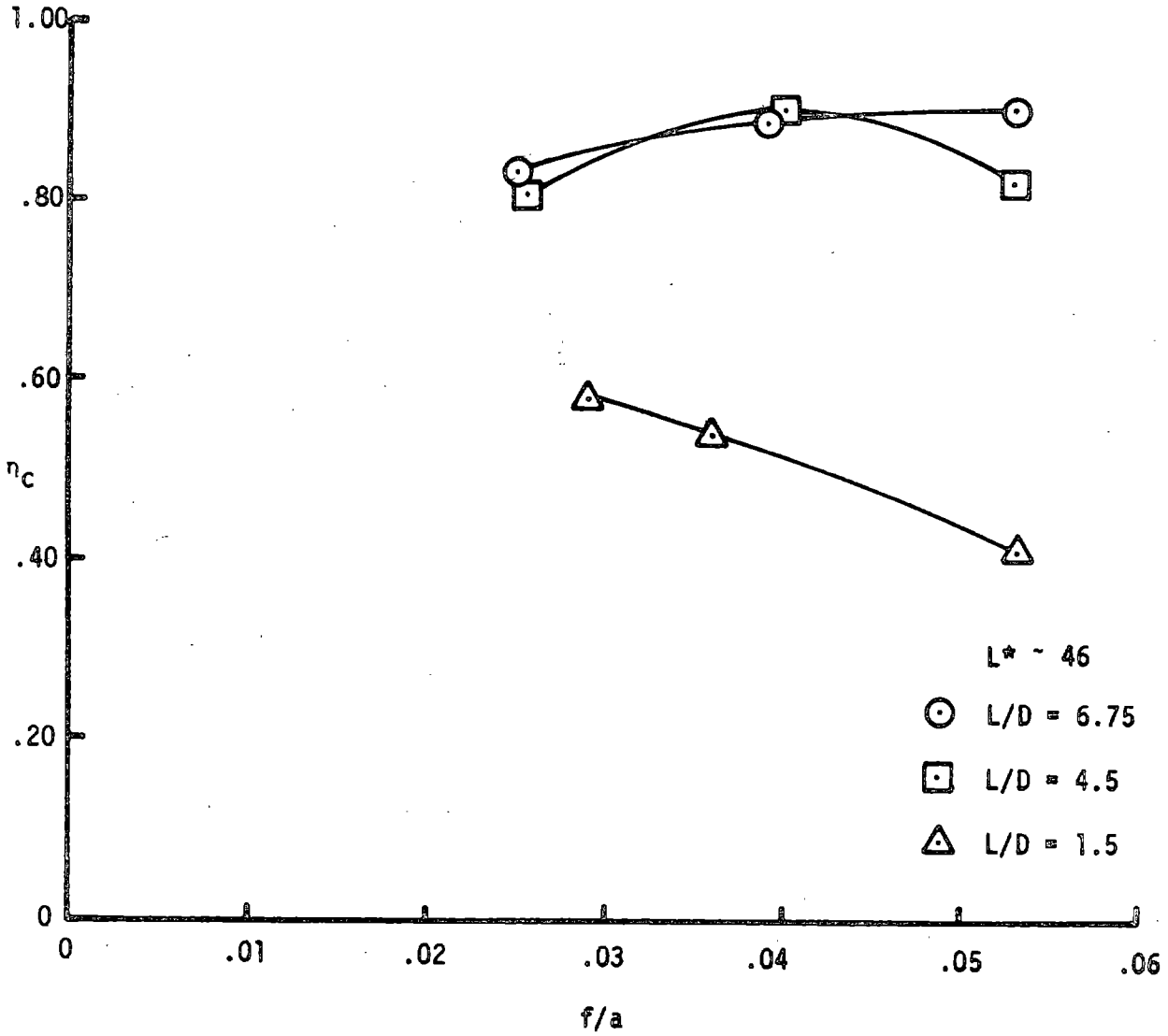

Figure 12. Constant Combustor L* Tests

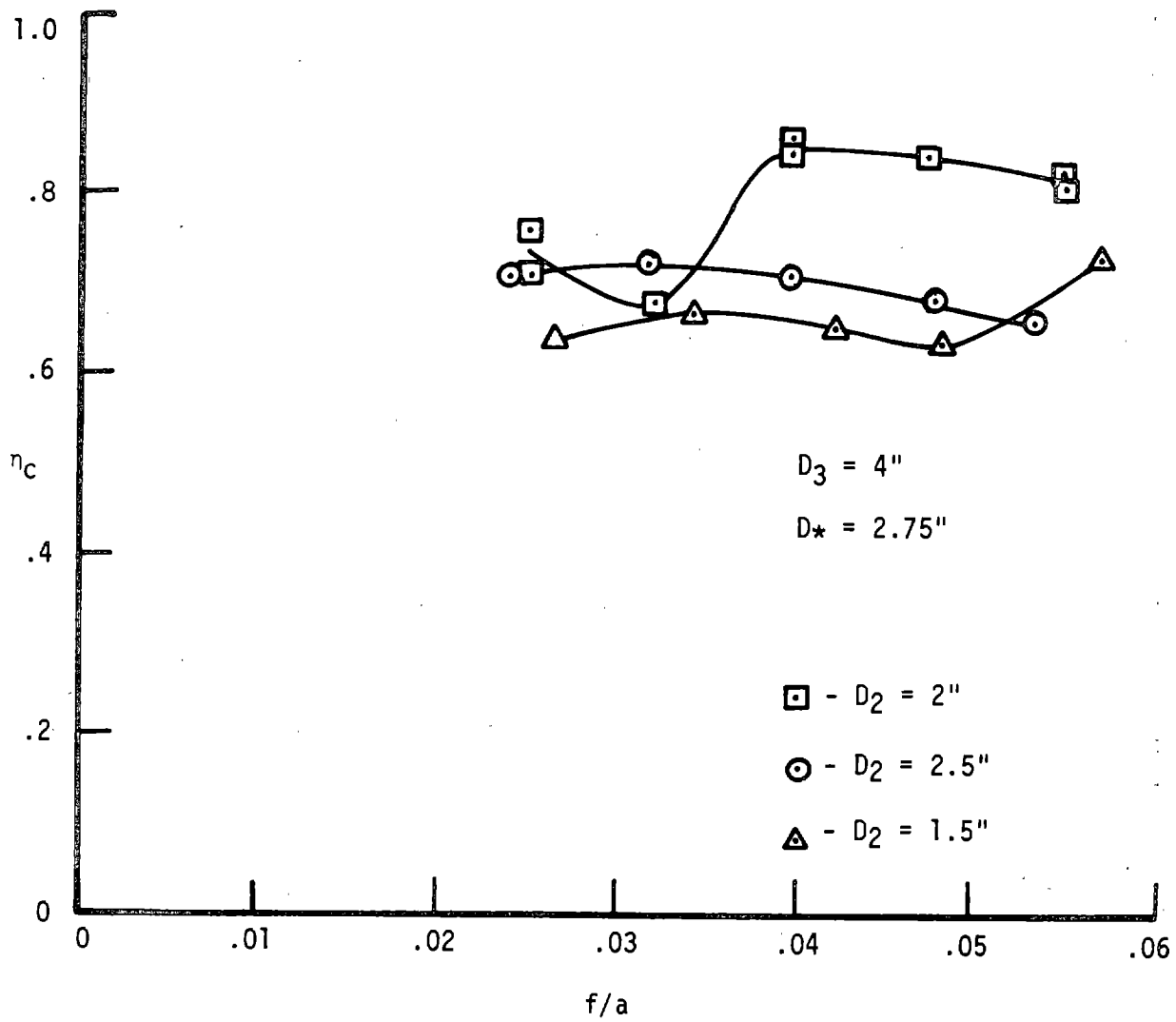

Figure 13. Effects of Dump Area Ratio

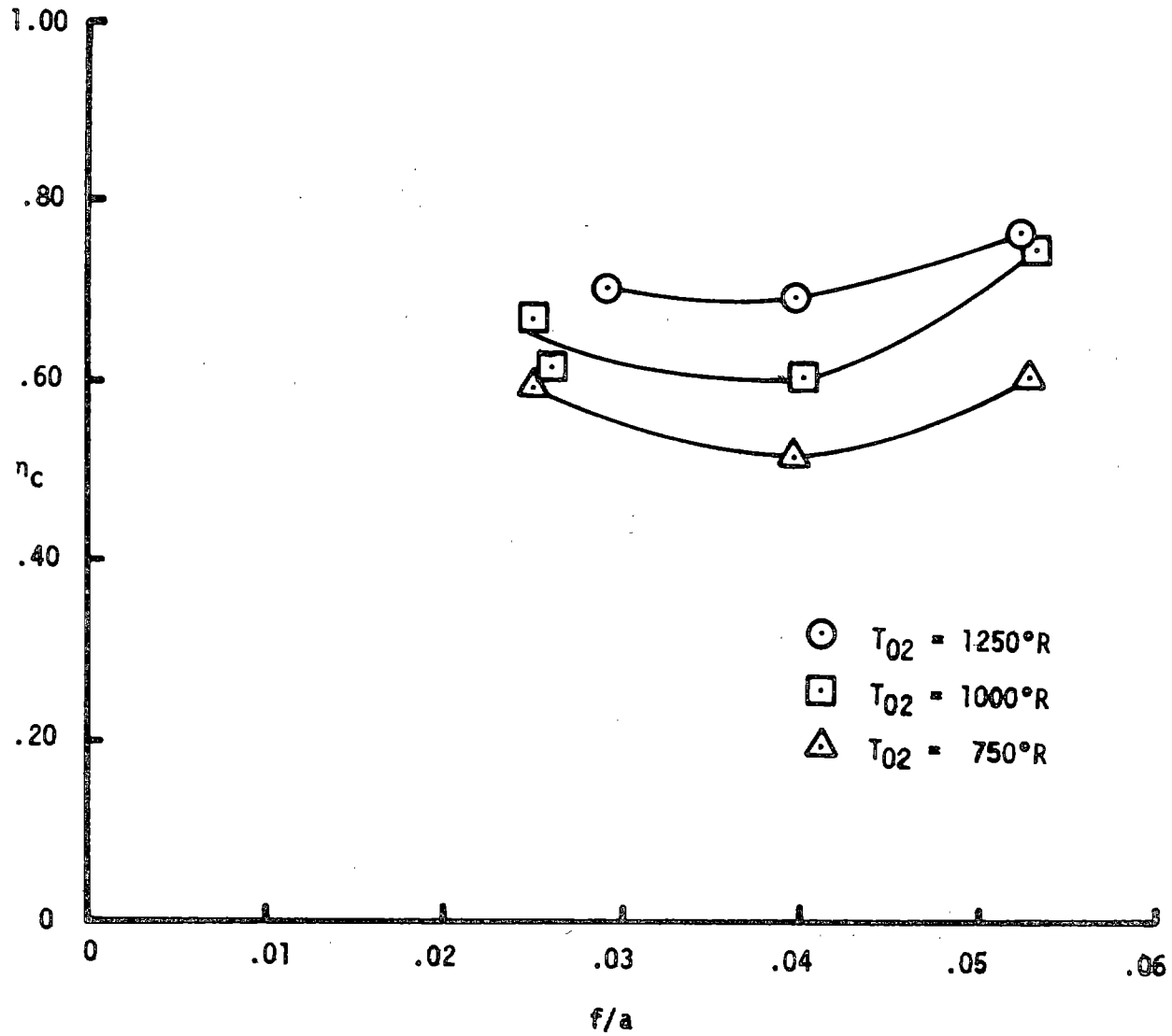

Figure 14. Effects of Inlet Air Temperature

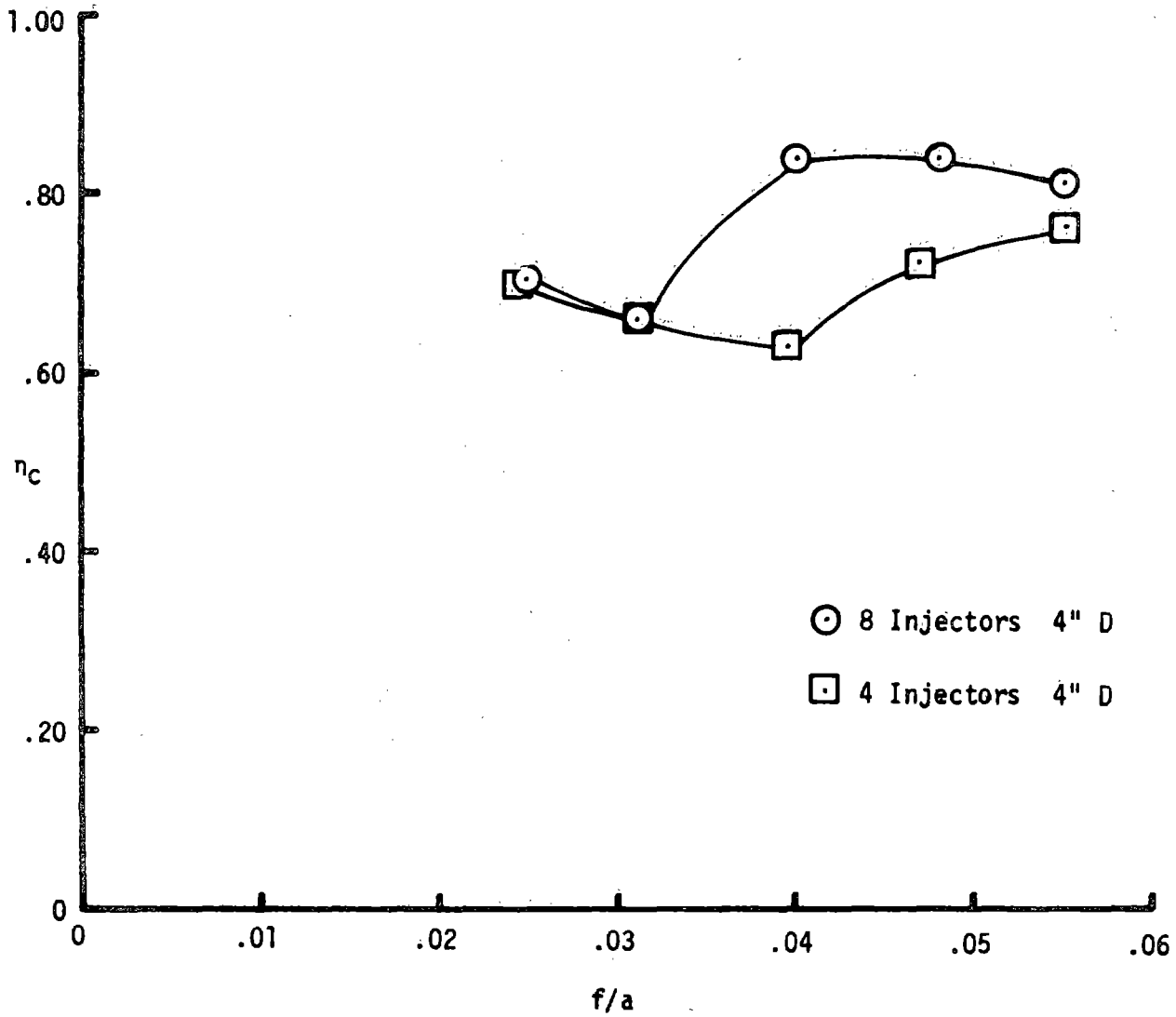

Figure 15. Effects of Injector Number

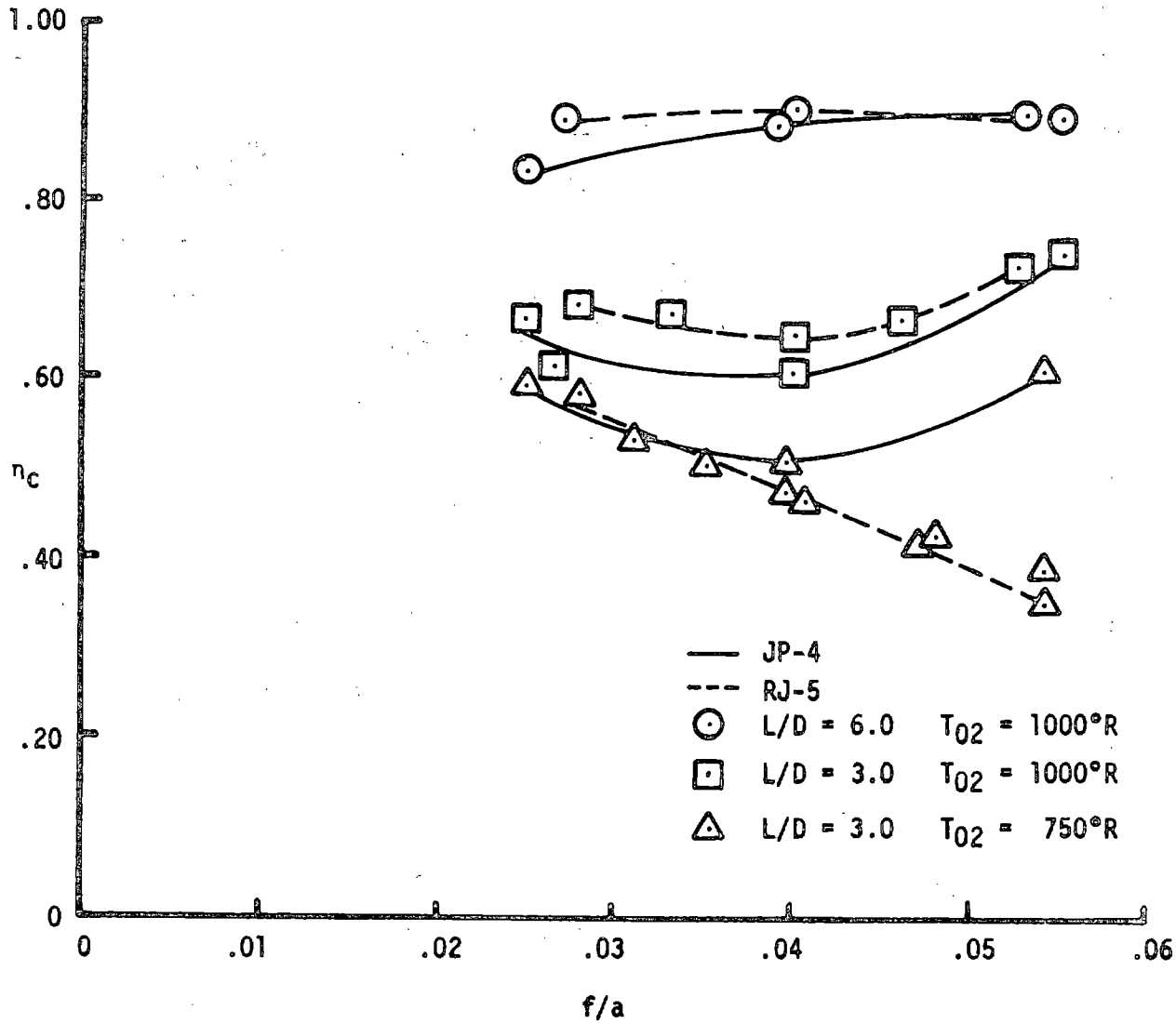

Figure 16. Effects of Fuel Type

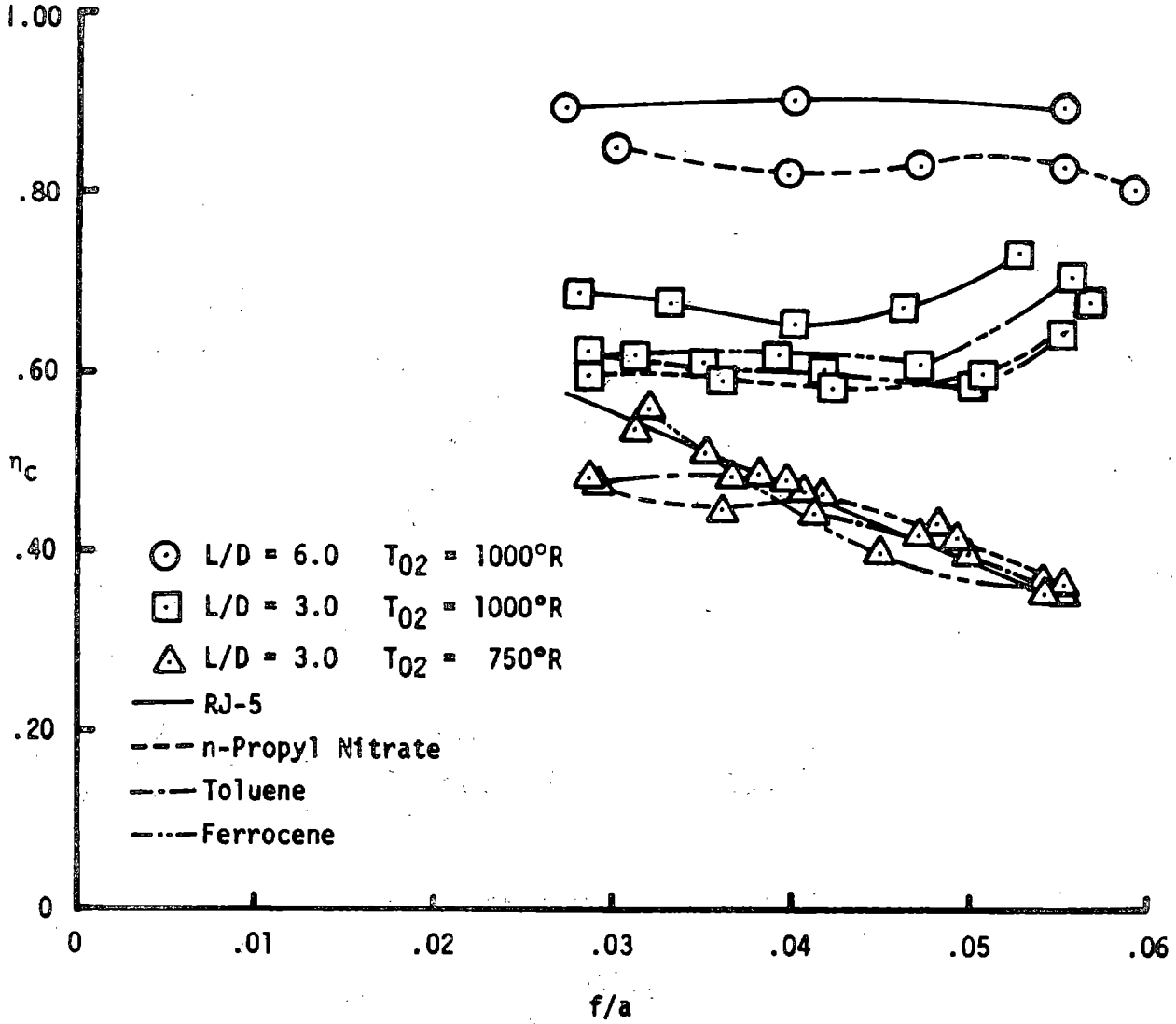

Figure 17. Effects of Fuel Additives to Shelldyne

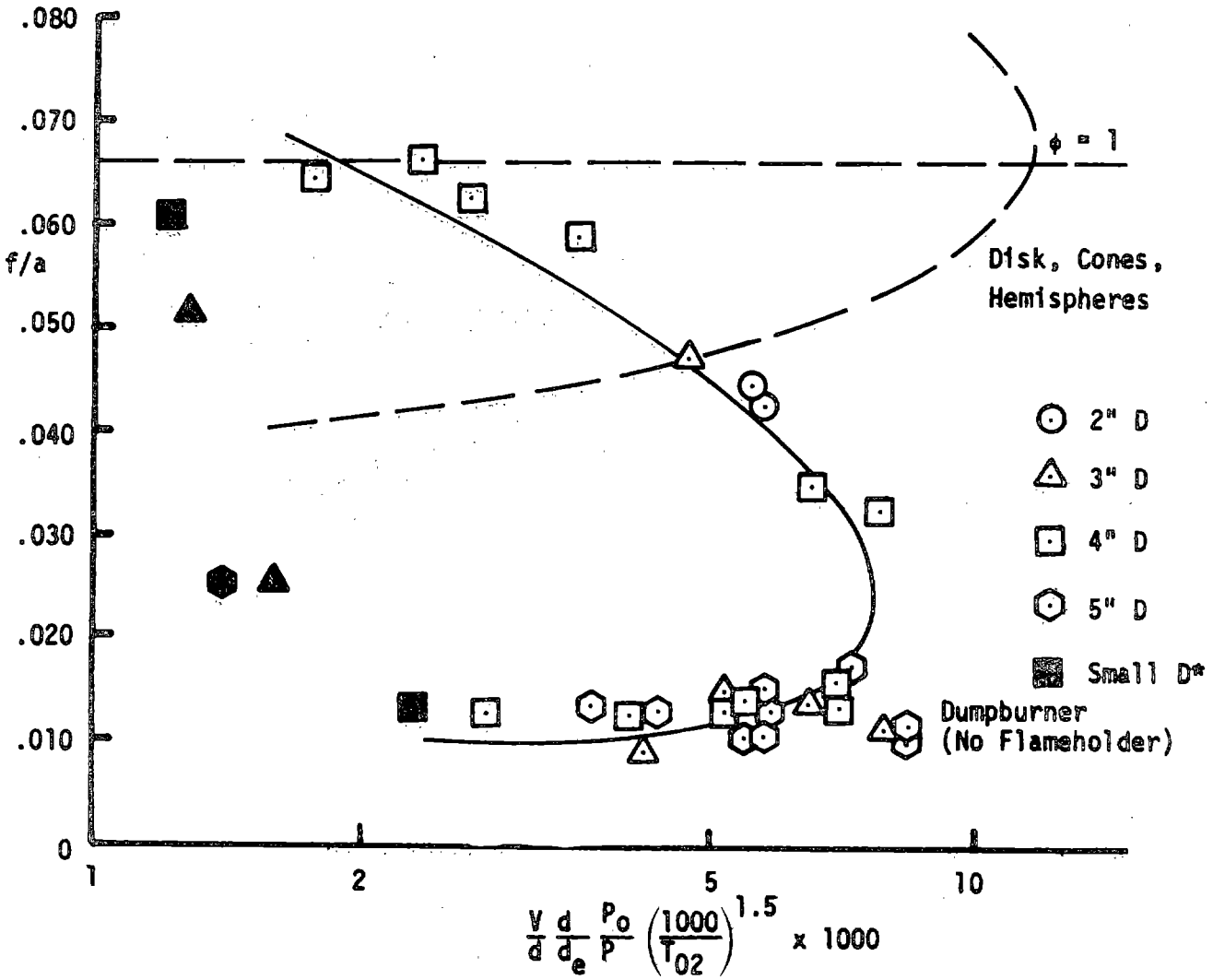

Figure 18. Stability Data Correlation

$$\frac{P^c\ A\ D^{.75}\ e^{T/b}}{W_A}$$ c & b → constants

$$\frac{V}{D}\ \frac{D}{d_e}\ \frac{14.7}{P}\left(\frac{1000}{T_{02}}\right)^{1.5} \times 12$$

$$L\left(\frac{D_4}{D^*}\right)^2 \frac{T_{02}}{1000}$$

$$\frac{W_A}{(Vol)P^2}$$

$$\frac{W_A}{A^*}\left(\frac{T_{02}}{1000}\right)^2 \times 144$$

$$\frac{P_{02}^{.324}\ T_{02}^{1.07}\ (750-U_2)^{.252}}{e^{a/L}}$$ a → constant

$$\frac{V}{P^{.95}\ D^{.85}}$$ $D \rightarrow \frac{D_3 - D_2}{2}$

$$\frac{4\ W_A}{\pi\ L\ (D^*)^2\ p^2} \times (12)^3(14.7)^2$$

$$\frac{V}{P\ D\ T_{02}^{1.7}}$$ $D \rightarrow \frac{D_3 - D_2}{2}$

Figure 19. Attempted Performance Correlations

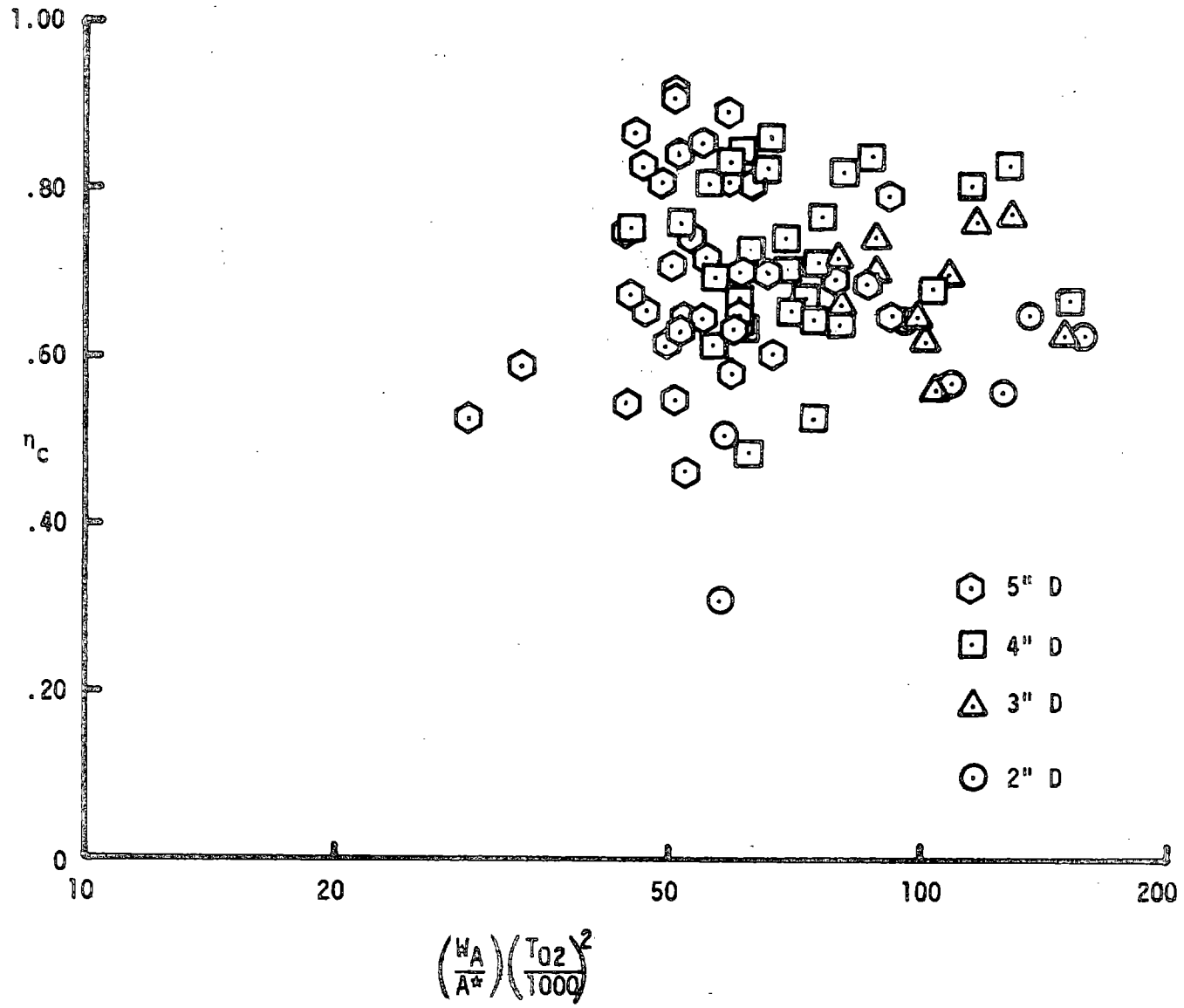

Figure 20. Burner Severity Parameter

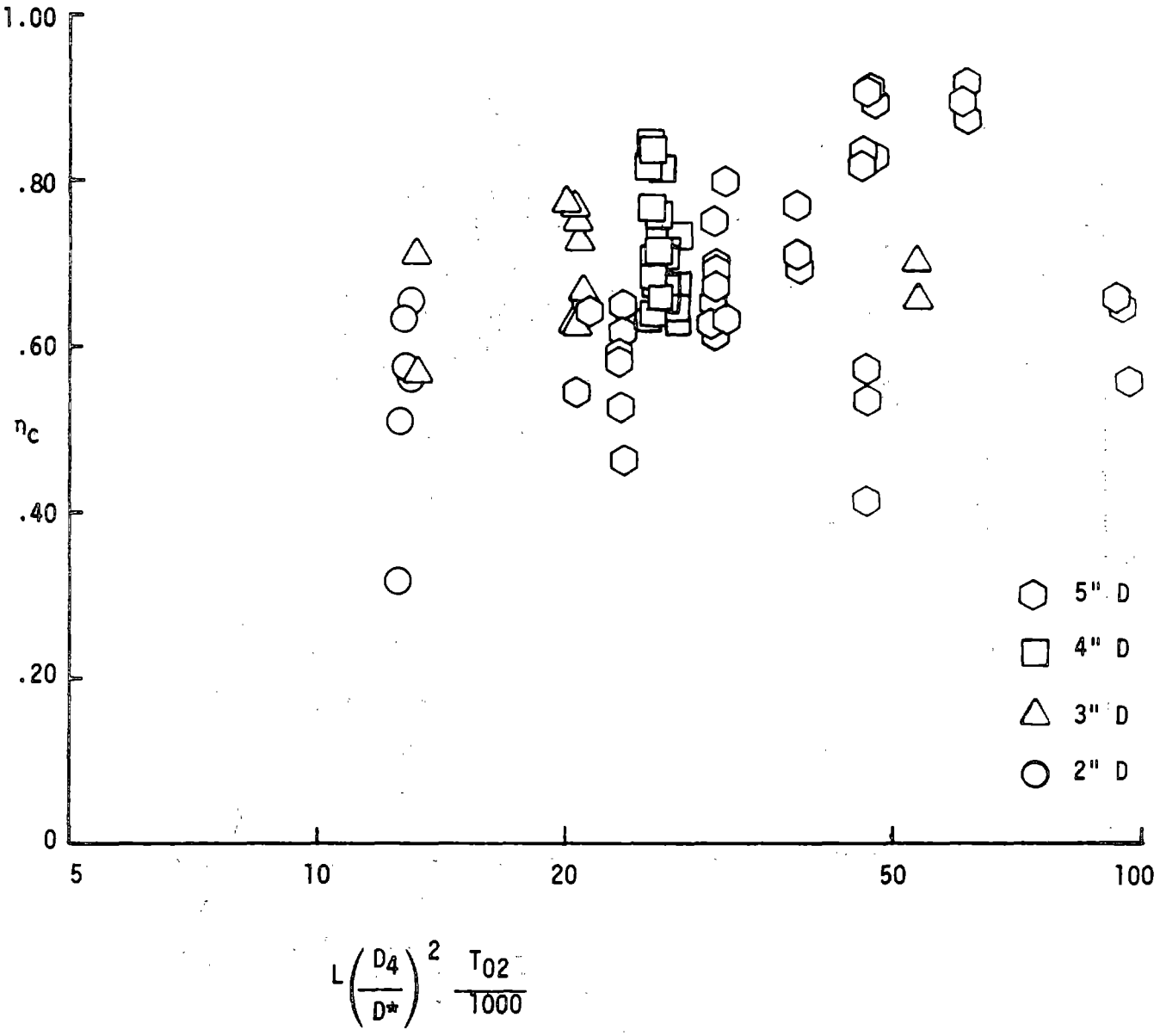

Figure 21. Characteristic Length Correlation

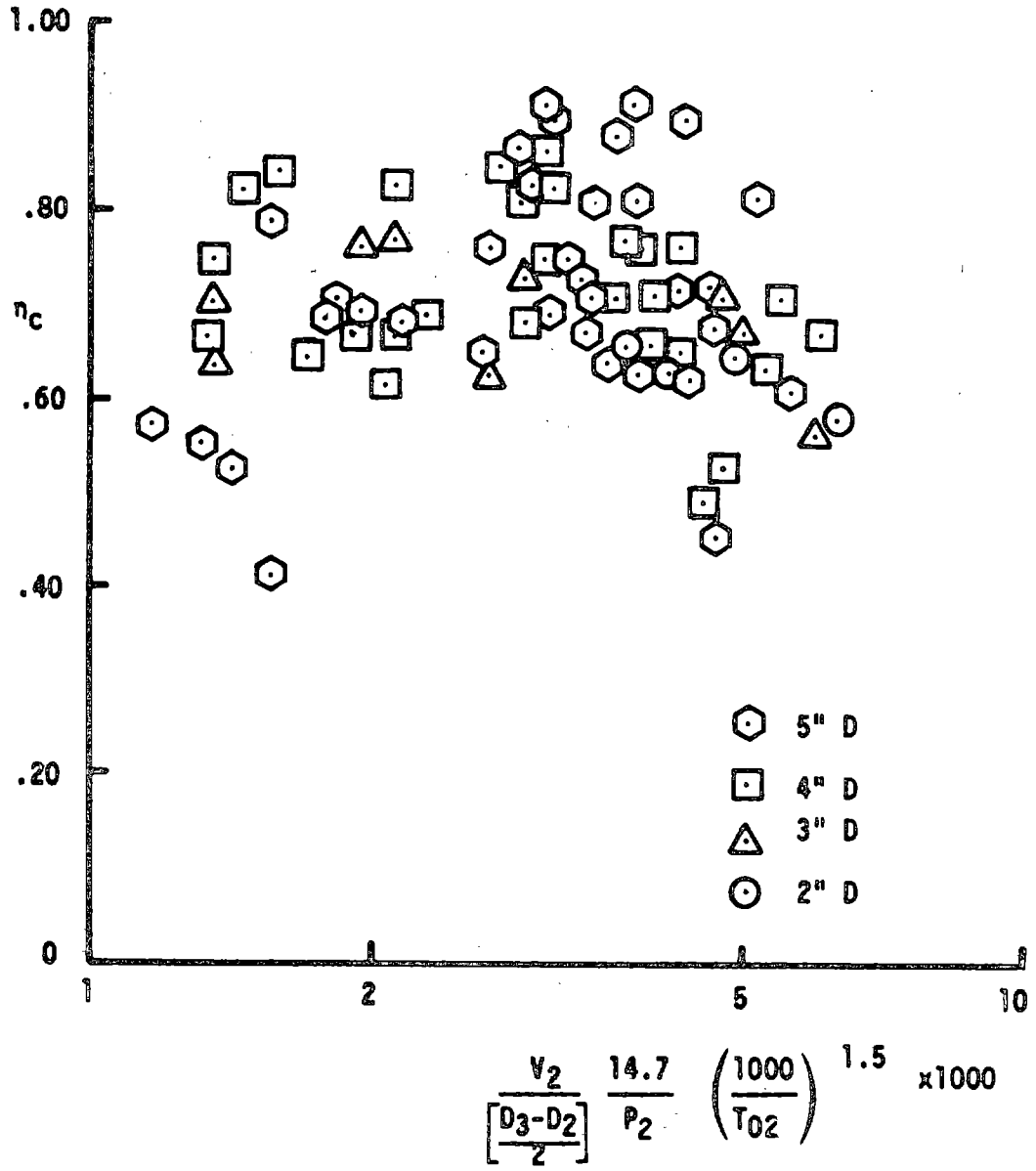

Figure 22. Stability Correlation

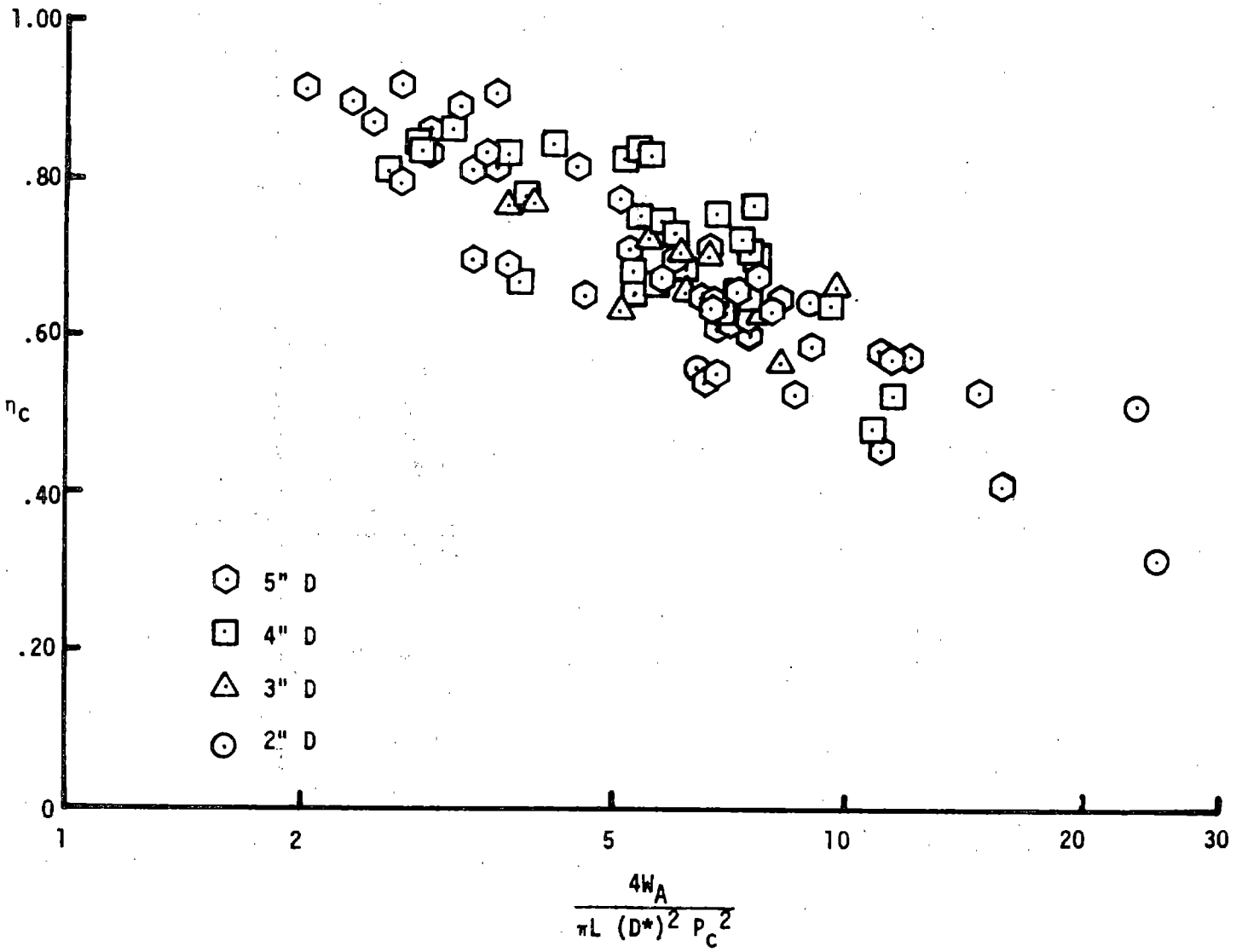

Figure 23. Modified Longwell Parameter

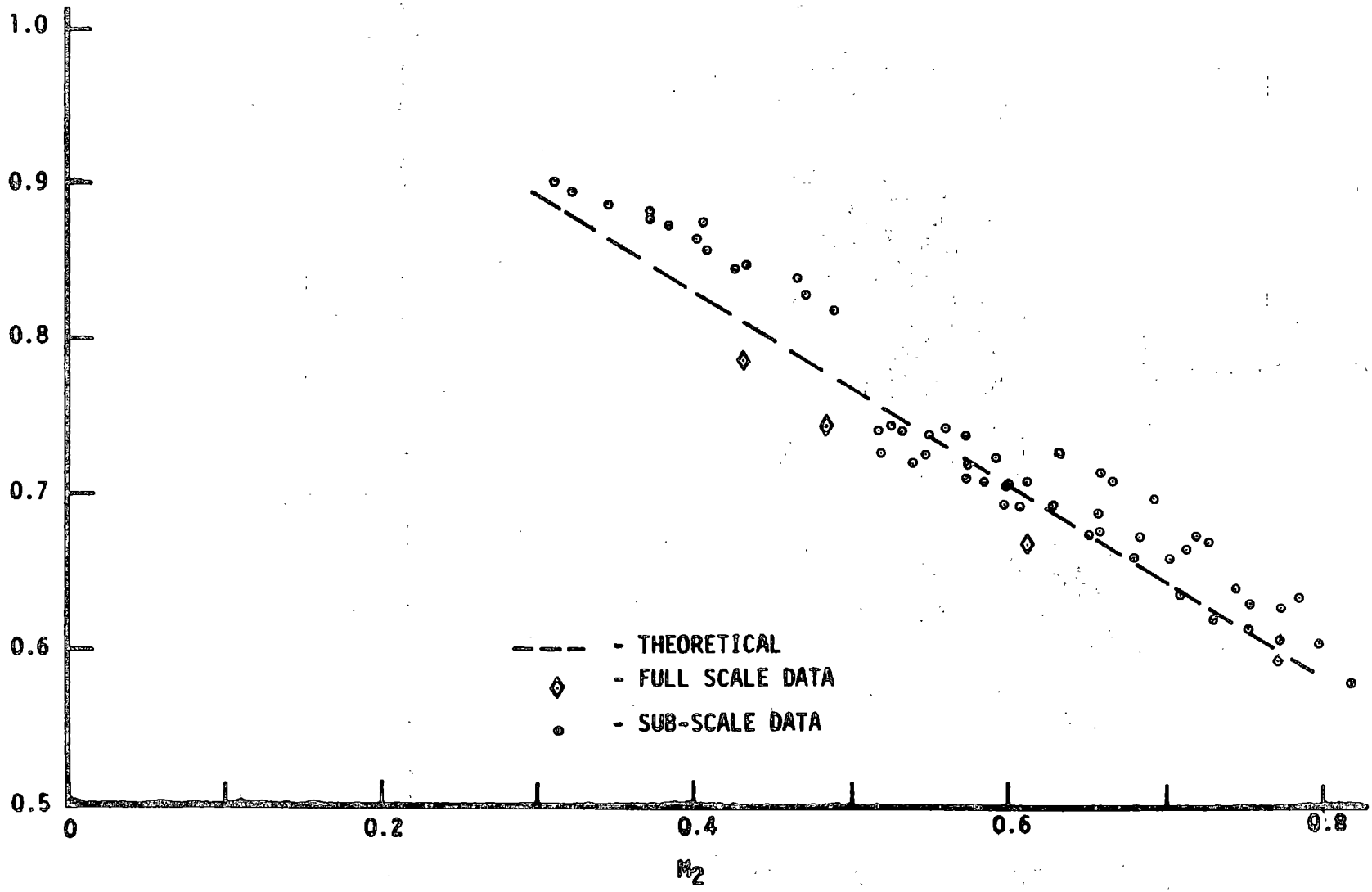

Figure 24. Pressure Loss Correlation Parameter

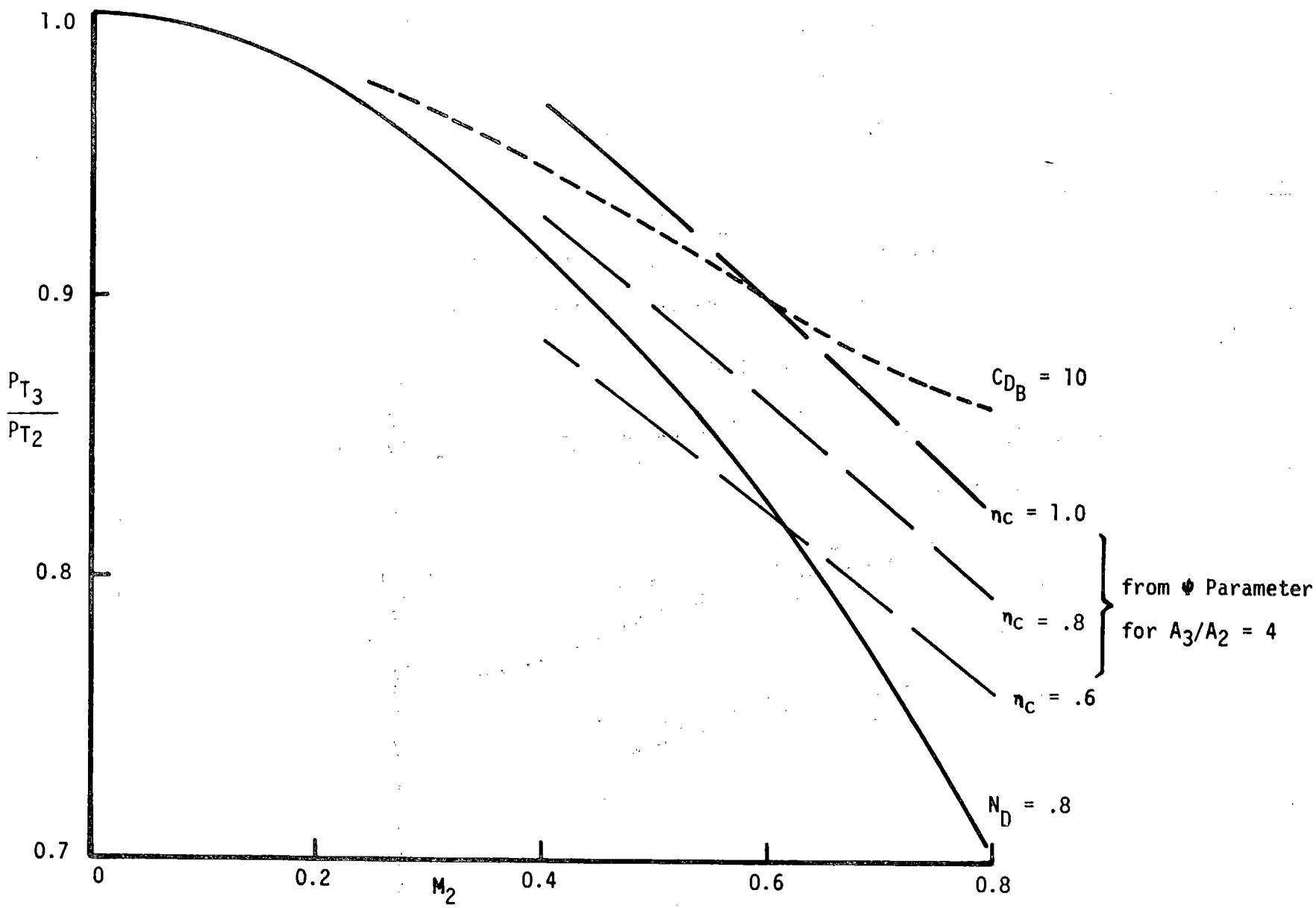

Figure 25. Comparison of Several Pressure Loss Parameters

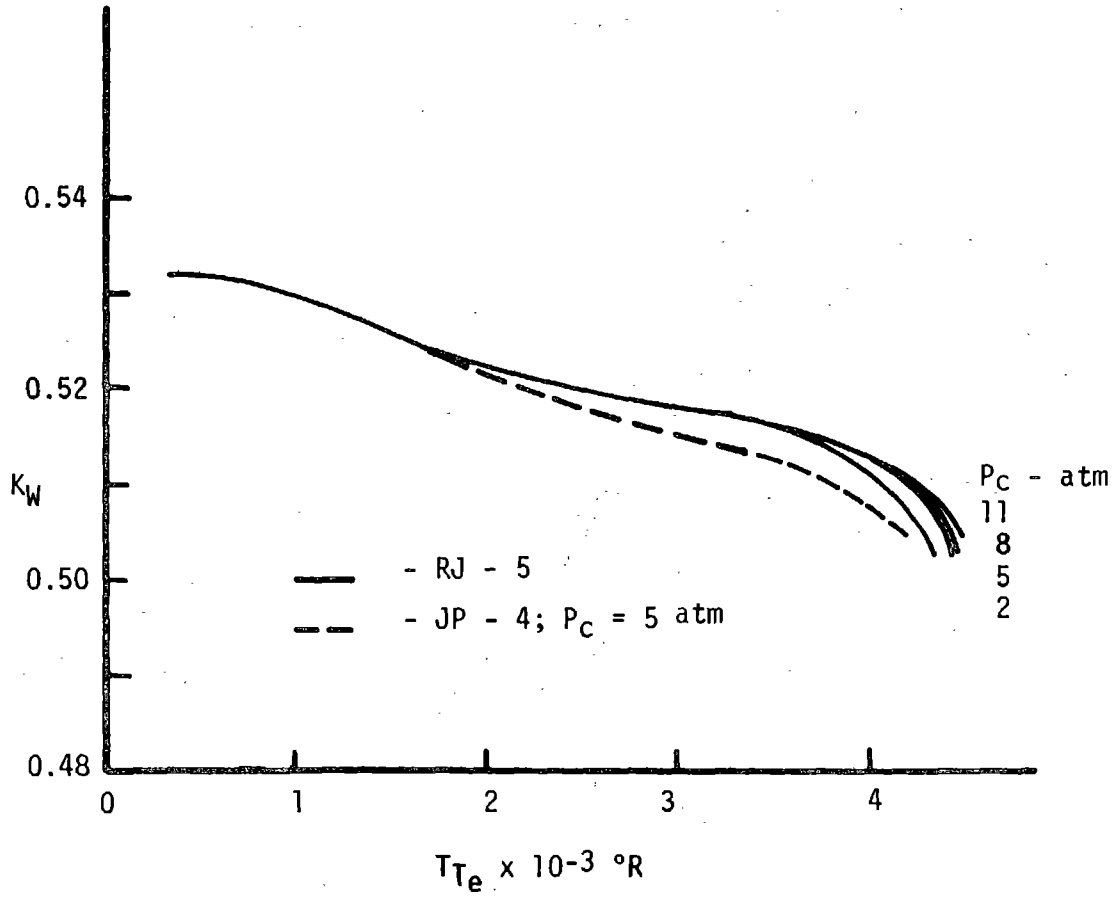

Figure 26. Mass Flow Parameter for Combustion Gases

☆U.S.Government Printing Office: 1974 — 657-016/319